

Catherine E. Deschênes

Environmental monitoring of microplastics using an unmanned vehicle and a hyperspectral imager

Proof-of-concept study for a more rapid sampling and analysis of surface marine microplastics

Master's thesis in Ocean Resources

Supervisor: Martin Wagner

Co-supervisor: Andrea Faltynkova and Artur Zolich

November 2023

Catherine E. Deschênes

Environmental monitoring of microplastics using an unmanned vehicle and a hyperspectral imager

Proof-of-concept study for a more rapid sampling and analysis of surface marine microplastics

Master's thesis in Ocean Resources
Supervisor: Martin Wagner
Co-supervisor: Andrea Faltnykova and Artur Zolich
November 2023

Norwegian University of Science and Technology
Faculty of Natural Sciences
Department of Biology



Catherine E. Deschênes

Environmental monitoring of microplastics using an unmanned vehicle and a hyperspectral imager

Proof-of-concept study for a more rapid sampling and analysis of surface marine microplastics



Master's thesis in Ocean Resources
Supervisor: Martin Wagner
Co-supervisor: Andrea Faltynkova and Arthur Zolich
November 2023

Norwegian University of Science and Technology
Faculty of Natural Sciences
Department of Biology



ABSTRACT

Marine plastics pollution is an urgent environmental matter. Understanding the transport and effects of plastics over long spatial and temporal scales must be a priority in environmental monitoring. Challenges from current methods have been addressed, including inadequate representation of real abundance, incompatibility between results, the necessity of a vessel for sampling, and time-consuming analysis.

This proof-of-concept study aimed to improve the sampling and analysis of microplastics (MPs) by combining a portable catamaran device (PCD) and a near-infrared hyperspectral imager (HSI). The PCD robot collected 35 samples over 4 days at two different locations around Runde, a bird-protected island on the Western coast of Norway - one location exposed to dominant current and wind, and the other protected. An HSI was used to increase sample analysis throughput and reduce time and costs. Environmental comparison of HSI was done using an attenuated total reflection Fourier transform infrared (ATR-FTIR).

We observed net advantages when using a robot combined with HSI, including increased accessibility, selectivity, scalability, and repeatability. HSI detected ($> 300 \mu\text{m}$) a significantly lower polypropylene (PP) concentration and a higher polyethylene (PE) concentration compared to ATR-FTIR. Higher abundance in a smaller size range was observed in both datasets. Overall, both HSI and FTIR methods effectively captured variations in MPs concentrations during the field campaign, with a mean of 0.09 MPs/m^3 , supporting the validity of HSI for detection. Significant variations of MPs concentrations between locations were observed with the HSI. At the exposed location, we observed the highest concentration and variation of MPs ranging from 0 to 0.79 MPs/m^3 . A positive correlation with wind speed likely explains the variations whereas tide levels were not correlated. Sampling over multiple days showed a significant difference in the medians between the days.

We conclude that sporadic MPs presence at Runde underscores the need for increased sampling frequency and addresses comparability limitations between studies. PCD and HSI can enable an easy repeatable sampling and analysis method for higher spatial and temporal variability to move towards a reproducible analytical pipeline for future MPs monitoring programs and understand better correlation between environmental factors and MPs concentration.

ACKNOWLEDGEMENTS

First, I would like to thank two very smart researchers without whom this project would have never been possible, my two co-supervisors: Andrea and Artur. Now both are officially parents of our beloved Pamela, aka the robot. Moreover, thanks to Martin and Andrea for all the support, guidance, and trust in undertaking this master thesis. Fieldwork and labwork would not have been possible without the warm and welcoming staff at Runde Miljøsentner and a special mention also to Grethe for the help and guidance in the lab, NTNU is truly lucky to have you!

Since I moved from Montreal to Trondheim, I have crossed paths with many incredible people, some with connections worth mentioning here as they contributed in unique ways to the success and completion of this thesis:

To my SoF gang thanks for making me fall in love with the Norwegian backcountry; To my girl gang and our cosy dinners; To my Svalbard women scientists who make me dream of a world ruled by more strong and independent women like you; To Njord, literally the best linjeforening in the whole world.

Little mention in french to all my people in Québec:

À la famille, merci infinément pour votre support éternel et constant malgré la distance. Je ressens votre amour jusqu'ici. Merci aux sentiments de réconforts à chacune de mes courtes et éphémères visites à maison, vous avez aucune idée à quel point je me sens choyée d'être si bien entourée; Merci à Menoum, vous m'inspirez toutes à votre façon; Merci à mes parents, grâce à vous, j'ai pu prendre le large pour mes études sans aucun soucis financier et j'en serai éternellement reconnaissante.

Finally, but not least, I want to acknowledge three people who made a difference in these last months of battle, and let's be honest, probably some depression here and there. My mom who without judgment guided me out of the black spiral I was in, towards the finish line; my grandpa, Papi, who has been my source of inspiration since day one, thanks for always believing in me; my partner in crime during this whole journey, Zoë, let's cheers to all the laughs, cries, deliriums, amazing and worse times of our lives: WE MADE IT!

CONTENTS

| | |
|---|-------------|
| Abstract | i |
| Acknowledgements | ii |
| Contents | iv |
| List of Figures | iv |
| List of Tables | vi |
| Abbreviations | viii |
| 1 Introduction | 1 |
| 1.1 Motivation | 1 |
| 1.2 Background | 2 |
| 1.2.1 Chemistry of plastics | 2 |
| 1.2.2 Plastics in the marine environment | 5 |
| 1.3 Challenges surrounding microplastic research | 7 |
| 1.3.1 Sampling of microplastics | 8 |
| 1.3.2 Analysis of microplastics | 9 |
| 1.3.3 Development of new technologies and methods for microplastic research | 10 |
| 1.4 Scope and objectives | 11 |
| 2 Methods | 13 |
| 2.1 Study area | 13 |
| 2.1.1 Sampling locations | 14 |
| 2.2 Fieldwork | 15 |
| 2.2.1 Sampling services and design | 15 |
| 2.2.2 Sample processing for transport and storage in Runde | 17 |
| 2.3 Quality assurance/quality control protocol | 17 |
| 2.4 Sample preparation in the laboratory at NTNU | 18 |
| 2.4.1 Soaking in soap for sample storage | 18 |
| 2.4.2 Fenton reaction | 19 |
| 2.4.3 Filtration | 20 |
| 2.5 Microplastics analysis and characterization | 20 |
| 2.5.1 HSI analysis | 20 |

| | | |
|----------|--|-----------|
| 2.5.2 | Microscope and FTIR analysis | 21 |
| 2.6 | Polyvinyl chloride spectral database implementation | 21 |
| 2.7 | Spatial and statistical analysis | 22 |
| 3 | Results | 23 |
| 3.1 | Methods performance | 23 |
| 3.1.1 | Portable Catamaran Device | 23 |
| 3.1.2 | HyperSpectral Imager | 25 |
| 3.1.3 | Improving HSI: PVC implementation in SIMCA model | 26 |
| 3.2 | MPs findings: environmental comparison of HSI with microscopy and ATR-FTIR | 27 |
| 3.2.1 | Quality Assurance and Quality Control | 27 |
| 3.2.2 | Abundance and Morphology of MPs: investigation of tech- nical and spatial differences | 28 |
| 3.3 | Diving in investigating the frequency of sampling and KEVs corre- lation | 32 |
| 3.3.1 | Frequency of sampling | 32 |
| 3.3.2 | Key environmental variables | 33 |
| 4 | Discussion | 38 |
| 4.1 | Methods Performance | 38 |
| 4.1.1 | Net advantage of using a robot and a hyperspectral imager compared to common methods used in MPs research | 38 |
| 4.1.2 | Addressing limitations: towards implementing reproducible analytical pipelines | 41 |
| 4.2 | Hyperspectral imager for environmental monitoring of microplastics | 43 |
| 4.2.1 | Analysis comparison and spatial differences: both instru- ments gave the same results, and the microplastic concen- trations may vary at different locations | 43 |
| 4.2.2 | Transport dynamics may influence spatial differences at Runde: exposed location contains a higher density of microplastics | 45 |
| 4.2.3 | Relevance of microplastics concentration detected at Runde compared to other studies | 45 |
| 4.3 | The relationship between key environmental variables, frequency of sampling, and microplastic concentrations | 47 |
| 4.4 | Outlook and future work | 49 |
| 5 | Conclusion | 50 |
| | References | 51 |
| | Appendices: | 62 |
| | A - Macro | 63 |
| | B - Statistical tests | 64 |
| | C - Fieldwork details | 65 |

LIST OF FIGURES

| | |
|---|----|
| 1.2.1 Overview of the sources, sinks, pathways and drifts of microplastics in the marine environment (Taken from Li et al. (2020) [66]). | 7 |
| 1.3.1 Global distribution of surface marine microplastics (MPs/m ³) with main ocean circulation (blue refers to cold, deeper water and red refers to warm, surface water). Data collected on 30.06.2023 from the marine database [67]). | 8 |
| 1.3.2 Reproducible analytical pipelines (RAPs) and technology readiness levels (TRLs) for microplastics (MPs) monitoring. a) shows the workflow for MPs research related to RAPs and b) shows the TRLs that need to be tested for each step in (a) Colors refer where the technology stands in terms of being able to be used for monitoring programs (Taken from Aliani et al. (2023) [85]). | 11 |
| 2.1.1 Sampling sites and the 35 runs at <i>location A</i> (680 m) and <i>location B</i> (600 m). <i>location A*</i> emphasizes the shorter path (370 m) used on Day 1 (2022-08-02). | 13 |
| 2.1.2 Fieldwork window in blue compared to tide and wind data two weeks before fieldwork. a) Tide data (m) per 20 min from Runde fyr and b) Wind data (m/s) per hour from Svinøy station (SN59800) | 15 |
| 2.2.1 Overview of the robot’s components and the equipment needed for fieldwork: a) displays all the principal components of the Portable Catamaran Drone (PCD) and equipment and b) shows a researcher carrying all the equipment provided by the sampling services to the fieldwork site | 16 |
| 3.1.1 Technical difficulties encountered during the fieldwork for specific transects at <i>locations A and B</i> . A normal trajectory is shown in each location as a reference. Ranges of yellow colors correspond to system issues whereas green colors correspond to physical issues | 24 |
| 3.1.2 Comparison of volume measurements taken from the flowmeter and the robot overall completed runs. The positively correlated linear regression trendline shows a significant difference between the measurements. Scatter-coloured dots correspond to all the completed runs used in this result section. | 25 |

| | | |
|-------|--|----|
| 3.1.3 | Comparison of the two methods, FTIR (green) and HSI (orange), using three artificial seawater spiked samples (SS1, SS2, SS3) as the true value (blue). Polymers, in known amounts from the spiked samples, are polyethylene (PE), polypropylene (PP), polystyrene (PS), polyethylene terephthalate (PET), polylactic acid (PLA). Count refers to the sum of plastic particles for each polymer in the spiked samples measured with the different instruments and compared to the true value. | 27 |
| 3.1.4 | Incorporating polyvinyl chloride (PVC) in the spectral database. a) Principal component analysis (PCA) scores plot comparing PVC plastics origin: C for consumer products and W for marine plastics and b) PCA scores plot comparing the different polymers from the spectral database with PVC | 28 |
| 3.2.1 | Polyoxymethylene (POM) spectral fingerprint from sample compared to a known contamination source using OpenSpecy [105]. a) Showing one of the spectral signatures of a fiber found in a sample, b) showing the spectral signature of the plastics material used for the 3D-printed ring, and c) a microscope picture showing a cluster of POM fibers | 29 |
| 3.2.2 | Distribution of MPs concentration (MPs/m ³) over the field campaign period comparing both locations and instruments used. | 30 |
| 3.2.3 | Comparison of MPs concentration per a) instrument (FTIR vs HSI) and per b) location (A vs B). Boxplot showing: interquartile range, minimum and maximum values, potential outlier, mean and SD of mean (red), and jitter of values per run are shown. | 31 |
| 3.2.4 | Comparing the polymer distribution of MPs for the two different analysis methods (FTIR vs HSI). PE: polyethylene, PMMA: polymethyl methacrylate, PP: polypropylene, PS: polystyrene. | 32 |
| 3.2.5 | Comparison of polyethylene (PE) and polypropylene (PP) concentration per a) and c) instrument (FTIR vs HSI) and per b) and d) location (A vs B). Boxplot showing: interquartile range, minimum and maximum values, potential outlier, mean and SD of mean (red), and jitter of values per run are shown. | 33 |
| 3.2.6 | Microplastics variation in shape depending on the instrument used: FTIR (green) vs HSI (orange) | 34 |
| 3.2.7 | Size of microplastics (MPs) quantified by FTIR and HSI | 34 |
| 3.3.1 | Comparison of microplastic concentration (MPs/m ³ per dates of field-work). Boxplot showing: interquartile range, minimum and maximum values, potential outlier, mean and SD of the mean (red), scatter dots coloured respectively by runs. | 36 |
| 3.3.2 | Investigation of microplastics (MPs) concentrations potential correlation to the key environmental variables (tide and wind speed). The trendline follows an lm model with standard error. | 37 |
| 3.3.3 | MPs concentration (MPs/m ³) compared to wind speed at Location A over the field campaign period. | 37 |
| C.1 | Examples of MPs detected by visual inspection under the microscope with the FTIR method but missed by the HSI method | 67 |
| C.2 | Colour distribution of samples analyzed under the FTIR method | 69 |

LIST OF TABLES

| | | |
|-------|--|----|
| 1.2.1 | Main plastics polymers, their density, and their common application. | 3 |
| 1.2.2 | Most commonly produced plastic polymers, and their chemical structure. | 4 |
| 1.2.3 | General shape categories related to microplastic classification. . . . | 6 |
| 1.3.1 | Common sampling equipment for surface water MPs research. . . . | 9 |
| 1.3.2 | Common analysis techniques used for microplastic identification and characterisation. | 10 |
| 2.4.1 | Samples and spiked samples distribution for the different batch processes in the laboratory. Some batches contain fewer samples because some samples were divided into separate vials because of a higher amount of organic matter in them. Analytical blanks from the laboratories in Runde and NTNU (B1a,b - B4a,b; A-G) and artificial spiked samples (SS1-SS3) | 19 |
| 3.3.1 | Fieldwork summary with the corresponding KEVs data: Location A corresponds to the exposed location and B to the sheltered one. Wind data was taken from Svinøy Station (SN59800) and tide data from Runde fyr. | 35 |
| 4.1.1 | Comparison of two other prototypes for MPs sampling to the one used in this study. All devices are trying to address current limitations related to the Manta Net. | 40 |
| B.1 | Statistical tests: p-value results (Signif. codes: 0 ‘***’ 0.001 ‘**’ 0.01 ‘*’ 0.05 ‘.’ 0.1 ‘ ’ 1) | 64 |
| C.1 | Summary of the field campaign including PCD information, MPs concentrations, and KEVs data related to each run. Yellow rows correspond to errors in the navigation system. Green rows correspond to entanglement with kelp in the propellers. | 66 |

ABBREVIATIONS

List of all abbreviations in alphabetic order:

- **ATR** Attenuated Total Reflectance Fourier-Transform Infra-Red
- **FPA** Focal Plane Array
- **FTIR** Fourier Transform InfraRed
- **GAM** Generalized Additive Models
- **GPS** Global Positioning System
- **HSI** HyperSpectral Imager
- **KEVs** Key Environmental Variables
- **LOD** Limit of Detection
- **LOQ** Limit of Quantification
- **lm** linear model
- **MPs** MicroPlastics
- **NAC** Norwegian Atlantic Current
- **NCC** Norwegian Coastal Current
- **NTNU** Norwegian University of Science and Technology
- **PCA** Principal Component Analysis
- **PCD** Portable Catamaran Device
- **PE** Polyethylene
- **PET** Polyethylene Terephthalate
- **PLA** Polylactic acid
- **PMMA** Polymethyl methacrylate
- **POM** Polyoxymethylene

- **PP** Polypropylene
- **PS** Polystyrene
- **PVC** Polyvinyl Chloride
- **Py-GC-MS** Pyrolysis-gas chromatograph-mass spectrometry
- **QA/QC** Quality assurance/Quality control
- **RAPs** Reproducible Analytical Pipelines
- **SD** Standard deviation
- **SIMCA** Soft independent modelling by class analogy
- **SS** Spiked samples
- **SDS** Sodium Dodecyl Sulfate
- **TRLs** Technological Readiness Levels
- **USV** Unmanned surface vehicle

INTRODUCTION

1.1 Motivation

In the past 100 years, the human population increased more than fourfold [1] which has given rise to a new geological epoch called Anthropocene, defined by Steffen et al. [2] as where "humans and our societies have become a global geophysical force". One of the major global threats from this era is marine pollution. Indeed, different contaminants in the marine environment have been studied during the last decades [3, 1]. The Anthropocene came with the industrialization and new perspectives towards more efficient productions [2], fewer constraints surrounding the economic growth of fossil fuels [4], and the innovation of a revolutionary synthetic material commonly called: Plastics [5].

As of 2021, the world plastics production stands at approximately 390.7 million metric tons (MMT) where 90.2 % is fossil-based and 44 % is used in packaging. In Europe, packaging also accounts for approximately 40 % of the total product share. Indeed, predicted growth scenarios of plastic waste entering the oceans compared to different mitigation strategies projected an annual emission of 53 MMT by 2030 in aquatic ecosystems from a Business As Usual model (BAU) [6]. Even if urgent and coordinated actions are implemented with current knowledge and technologies, a 78 % reduction of the BAU plastic pollution rates by 2040 would still lead to a massive accumulation of plastics in the environment because of their long residence times [7]. Thus, plastics pollution is a major concern for humanity as it can have a serious impact on biodiversity [8, 9] and food security [10].

An urgent shift towards more sustainable food resources from the ocean is needed [11] as the world population keeps increasing [12]. There is a clear call for healthy and clean marine ecosystems to ensure the resilience and productivity of marine resources [11]. As an example, Walkinshaw et al. [13] reported that 50-75 % of the common fishes from aquaculture and fisheries had ingested plastics. Thus, marine plastics pollution is ubiquitous in different aquatic environments of the world [8, 1, 14, 9]. From deep sea sediments [15, 16, 17] and ocean trenches to surface accumulation in ocean gyres [18, 19], it varies spatially within the biosphere and can be transported even to the most remote and pristine places where human-

1. INTRODUCTION

ity have left little or none of its fingerprint [20, 21, 22]. Consequently, plastic pollution has reached an alarming extent among marine species, impacting them through various mechanisms such as entanglement [23, 24] and ingestion [25, 26] affecting a wide range of organisms from marine mammals to phytoplanktons [8, 14, 13]. Hence, bioconcentration [27] and trophic transfer [25, 28] raises concerns for human health [29] as plastics have already been discovered in human blood [30].

Overall, only a glimpse of some environmental impacts of plastic pollution has been mentioned. It is important to underscore the additional repercussions of plastic disposal. From wonder to criticized material, plastics, if not ending up in the ocean, are mainly burned, recycled, exported, or buried at the end of their life which results in a waste of energy and resources, especially for single-use plastics [8]. Indeed, plastics production, from cradle to grave, can also have an unprecedented effect on climate change due to its significant carbon footprint related to the release of greenhouse gas (GHG) associated with fossil-fuel extraction and energy required to produce virgin plastics [31]. Hence, plastics pollution needs to be addressed with multidisciplinary approaches as its effects are only adding to stressors that the global biosphere is already struggling with [32, 33, 1, 34]. The first step, as a young researcher and scientist in the field, is to aid and standardize plastic research to create and fortify the bridge between researchers, politicians, stakeholders, and citizens.

1.2 Background

Molecules consisting of a high number of repeating building blocks, or monomers, linked together by covalent bonds are called polymers. Through polymerization, these polymeric chains contain enough repeating units so that their physicochemical characteristics do not change significantly when subsequent units are added. Their large molecular weight permits them to entangle with each other and resist more easily to breakage. Polymers are naturally occurring in the environment since life began. Indeed, DNA, cellulose, cotton, wool, silk, and rubber are a few examples of extracted polymers from nature. No wonder humans would eventually create synthetic polymers to mimic their strength, flexibility, resistance, and versatility [35, 36]. Through polymerization or polycondensation, some synthetic polymers, referred to as plastics, are derived from petroleum or natural gas rendering unique monomers with different functional and structural properties.

1.2.1 Chemistry of plastics

Plastics, being synthetic polymeric compounds exhibit distinct chemical properties due to variations in their architecture, molecular weight, melting point, and crystallinity levels [37, 38]. Derived from fossil feedstocks, the monomers forming the polymer chains play a crucial role in classifying plastics based on their chemistry and properties, designed for specific applications.

A key distinction lies in the forces between polymer chains, with strong covalent bonds making thermosets resistant to melting, softening, and bending. Thermoplastics, on the other hand, can be melted and moulded repeatedly, categorized

1. INTRODUCTION

as amorphous or semi-crystalline, from a less to a more structured order or energy needed to melt the material. Indeed, the degree of crystallinity, influenced by the polymer chains' tacticity, the 3D arrangement of carbon, will dictate the energy needed for melting. Functional groups, within the chemical structure of a monomer, are mainly responsible for these overall characteristics, influencing the chemical properties and behaviours of plastics, that help us distinguish between different plastic polymers. Hence, they are impacting significantly the density, the crystallinity, and the glass transition temperature of the polymer. By increasing the crystallinity, density also increases due to packing of the polymer chains closer together. Additionally, functional groups determine the glass transition temperature which marks the threshold for flexibility and impacts the resistance in plastics (Table 1.2.2). Overall, functional groups and backbone chemistry of the different plastic polymers will contribute and shape their behaviours under various conditions [36, 39, 35].

The major categories of polymers are shown here in Table 1.2.1. Chemical structure and functional groups on five of the most common plastics produced in Europe [40] (see Table 1.2.2).

Table 1.2.1: Main plastics polymers, their density, and their common application.

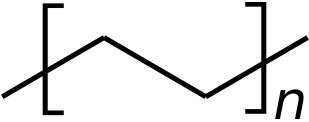
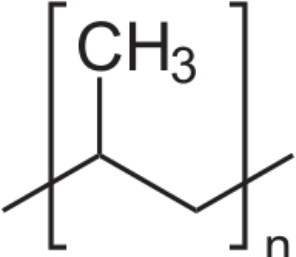
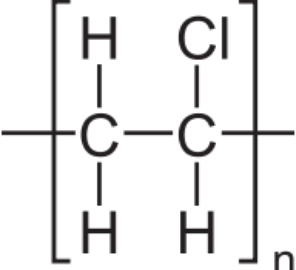
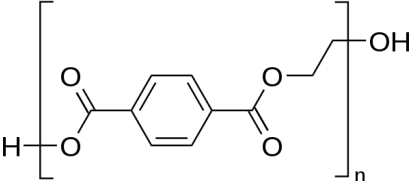
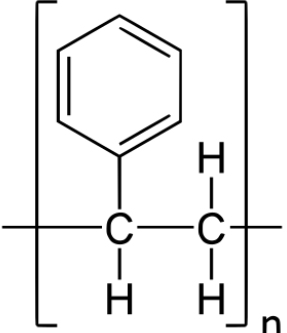
| Polymers | Density (g/cm^3) | Application |
|--|-----------------------|---|
| Semi-crystalline thermoplastics | | |
| Polyethylene (PE) | 0.89-0.99 | Packaging, building, and aquaculture/fisheries |
| -Low-density PE (LDPE) | 0.91-0.93 | Films, bags, and nets |
| -High-density PE (HDPE) | 0.94-0.97 | Containers (Jars, flasks, caps) |
| Poly(ethylene terephthalate) (PET) | 1.33-1.42 | Bottles |
| Polypropylene (PP) | 0.85-0.92 | Rope, caps, containers |
| Polyamides or Nylon 6 (PA) | 1.12-1.24 | Textile |
| Poly(oxyethylene) or polyacetal (POM) | 1.40 | Automotive, electronics, building, engineering resins |
| Polyester (PES or PET) | 1.39 | Synthetic fibers, films |
| Amorphous thermoplastics | | |
| Polystyrene (PS) | 1.04-1.09 (Foam 0.05) | Packaging, insulation |
| Poly(vinyl chloride) (PVC) | 1.37-1.44 | Packaging, pipes, cables |
| Poly(methyl methacrylate) (PMMA) | 1.16-1.20 | glass alternative |
| Thermosets | | |
| Alkyd varnish | 0.9-0.19 | surface coating resin |
| Phenoxy resin | 1.18 | Flexible/rigid coatings for adhesion or composites |

Source: Andrady 2022 [8], Grigorescu et al. (2019) [41], Rudolph et. al. 2017[42], Sastri 2010 [43]

More than 10,000 different chemical substances have been found for plastic polymers [44, 45]. Indeed, plastic materials, formed through polymer modification or compounding, involve blending diverse additives to meet the specific application it should be used for. These additives, including fillers, plasticizers, antioxidants, and flame retardants, enhance plastic performance and processing. For instance, fillers are used to add stiffness and hardness to plastic; stabilizers can help prevent oxidation under heat or exposure to sunlight; aids, agents, and lubricants are used during processing and polymerization [46]. Despite their widespread use, they pose environmental and health risks upon human and organism exposure. Many additives are persistent bioaccumulative toxic chemicals, known as endocrine-disrupting chemicals (EDCs) and persistent organic pollutants (POPs).

1. INTRODUCTION

Table 1.2.2: Most commonly produced plastic polymers, and their chemical structure.

| Polymers | Monomer's chemical structure | |
|----------|-----------------------------------|---|
| PE | C-C backbone on ethylene monomer |  |
| PP | C-C backbone on propylene monomer |  |
| PVC | chloride as functional groups |  |
| PET | ester as functional groups |  |
| PS | phenyl as functional groups |  |

Source: Plastics Europe 2022 [40]

1. INTRODUCTION

Common EDCs like phthalates, bisphenol-A (BPA), and polybrominated diphenyl ethers (PBDEs) can have adverse effects on reproduction and development. POPs, such as polychlorinated biphenyls (PCBs) and polycyclic aromatic hydrocarbons (PAHs), persist in the environment, causing harmful effects on the immune system and overall health [44]. All plastic polymers presented in Table 1.2.1 are associated with one or multiple of these additives.

Overall, plastics' versatility and ubiquity in the environment are due to their numerous applications and variety which is why a high number of plastic additives have been added to the Norwegian priority list of hazardous substances [47] due to rising concerns about their environmental impact. More recently, during negotiations for the Global Plastic Treaty, chemicals in plastics should be an integral part of it to be effective in producing accurate solutions [48].

1.2.2 Plastics in the marine environment

Sources, distribution, and transport of plastics in the marine environment are affected and governed by many factors. Smaller plastics, called microplastics (MPs) in marine environments can come from two different types of sources: primary or secondary MPs. Primary MPs are introduced directly in the marine environment from plastic industry runoffs, transport or cosmetics products whereas secondary MPs are from fragmentation of plastics due to external factors and forces that act on it.

Indeed, the weathering of plastics in the marine environment is caused by several drivers. The surface and bulk phases of plastics can change mechanically and morphologically when impacted by abiotic and biotic weathering. Photooxidation while decreasing the hydrophobicity of the polymer, can also increase its crystallinity by altering the amorphous regions of the polymer. Hence, even without any additional mechanical stress, the brittleness of the plastic from the sun radiation can increase fragmentation [38, 49]. Further biotic weathering can then occur, such as biofouling including biofilm formation and bacteria mineralization and/or marine organisms ingestion and, therefore, digestion. Hence, this transformation makes the weathered plastic readily available for uptake by organisms as they can be confused for natural prey because of their similar size and biofilm coating [38, 8, 49]. The concept of a "plastisphere" associated with MPs has emerged, investigating its significance in the degradation and adsorption of pollutants [50].

The risk of biomagnification and bioaccumulation of MPs in the food web is alarming as MPs toxicity is studied across numerous marine biota [51]. Indeed, marine sentinel species like seabirds [52] and marine mammals [23, 34] have been affected by MPs. For instance, evidence of MPs presence in feeding grounds of manta rays and whale sharks and estimating ingestion rates from 25 to 137 pieces/h [53]. Inevitably, it was only a matter of time for MPs to reach humans [29], as seen in human blood samples for instance [30].

A pragmatic definition for MPs was decided at the first international workshop hosted by NOAA where the upper boundary was set to 5 mm in size [54]. It was initially to distinguish the ingested plastics marine debris from the larger items that can cause entanglement [55]. Furthermore, in most field studies, MPs

1. INTRODUCTION

Table 1.2.3: General shape categories related to microplastic classification.

| Shape | Description |
|----------|--|
| Pellet | spherical, primary origin |
| Film | thin, soft, often transparent, 2D rectangle |
| Fragment | hard, irregular, color variable |
| Fiber | narrow and long strands from textile or ocean industries |

Source: Löder and Gerdts (2015) [61], Fiore et al. (2022) [62]

refer to particles found in the environment larger than 300-500 μm because of the common sampling methods used where the limit of detection (LOD) is restricted by common sampling practices (neuston or manta trawls). Nowadays, with the addition of a new size class called "nanoplastics" (NPs) corresponding to any particles lower than 1 μm . Particles longer than 5000 μm are in a size class called "mesoplastics" with MPs being in the middle with a size range variable depending on the limitations of the sampling and analysis methods used.

Important physical characteristics are size, shape, and colour. Environmental plastics vary in these morphological properties as soon as they start to disintegrate and reduce in size with irregular, and more unique, geometries. Size is one of the main parameters for plastic classification as it dictates their mobility in seawater and how they interact with the marine biota. However, the shape is also important to report as it plays a major role in the dispersion of plastics in seawater [56, 57]. Shapes within MPs vary depending on the identification used. Visual and microscopic classification leads to higher classifications of particles whereas others have less. Frias and Nash (2019) [58] reported ten different categories of shape whereas other studies only reported four [59, 60, 57]. Common shape categories are described in Table 1.2.3.

Finally, the analysis of colours can provide useful information on the source of plastics and, for instance, noticing sample contamination. However, its effectiveness becomes increasingly arbitrary and challenging as the size of the plastics decreases and their residence time in the highly dynamic marine environment extends.

Released MPs have dynamic interactions with the coast since they are influenced by onshore and offshore transport which are in turn governed by hydrodynamic processes specific to the source location as well as physical parameters and biochemical interactions [63] (see Figure 1.2.1). Moreover, abiotic and biotic factors transport processes are affecting and complicating the distribution and prediction of MPs in the marine environment. Settling behaviour to the sediment is influenced by MPs shapes and sizes as well as any biofilm interaction and aggregates formation [50, 49]. Turbulence by currents and waves can influence low-density MPs by dragging and drifting the particles increasing their exposure to shear stress and their resuspension in the water column [49, 64, 65]. Hence, secondary MPs formation is most likely to occur in warmer waters of the coast due to the combination of photooxidation and shear stress from shorelines.

1. INTRODUCTION

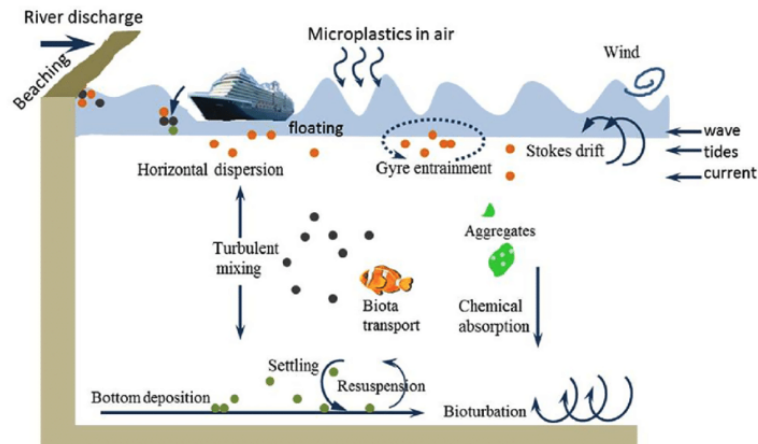


Figure 1.2.1: Overview of the sources, sinks, pathways and drifts of microplastics in the marine environment (Taken from Li et al. (2020) [66]).

Overall, the ubiquity of MPs is unprecedented and studies surrounding the topics have exponentially grown in the past decades. While plastic pollution has also increased in tandem with rising plastic production, we have come to recognize the alarming and persistently slow residence time in the marine environment. The need to gather as much data as possible to understand the problem and provide solutions is utmost urgent. However, reproducibility and repeatability of data are hard when no standard or common methods are in place.

1.3 Challenges surrounding microplastic research

Marine plastic pollution is an urgent environmental matter [9] as the ubiquity of MPs in the ocean is more and more concerning every day [68, 69, 1, 14]. While solutions driven by guidelines and monitoring framework should have already been in place yesterday [55, 70, 71] as MPs research is investigated globally (Figure 1.3.1, challenges and limitations including lack of standardized methods and limited throughput on spatial and temporal scales are persisting which affects the reproducibility and comparability of MPs data effectively [72]. With all this data available, there is an urgent need for any proper comparable and reproducible guidelines in place to answer specific questions with the appropriate methods about the heterogeneous array of MPs in size, unique shapes from weathering, and colours [73].

Quantifying MPs in the marine environment is normally done following four steps: sample collection, separation, analysis, and quality assurance/quality control (QA/QC). For sample collection and separation, the matrix chosen will dictate the methods used. Separation of MPs is often done using density separation, enzymatic treatment, and/or wet peroxidation to remove the organic matter from the sample [74]. For sample analysis, it will be independent of the matrix, but more dependent on the size of MPs related to a specific research question, based on the instrument available to the researcher, and the researcher's expertise. The determination of the size of MPs can also be a limitation introduced while sampling or using sieves during the separation step. Cost-effective method standardization and

Marine Microplastics Distribution

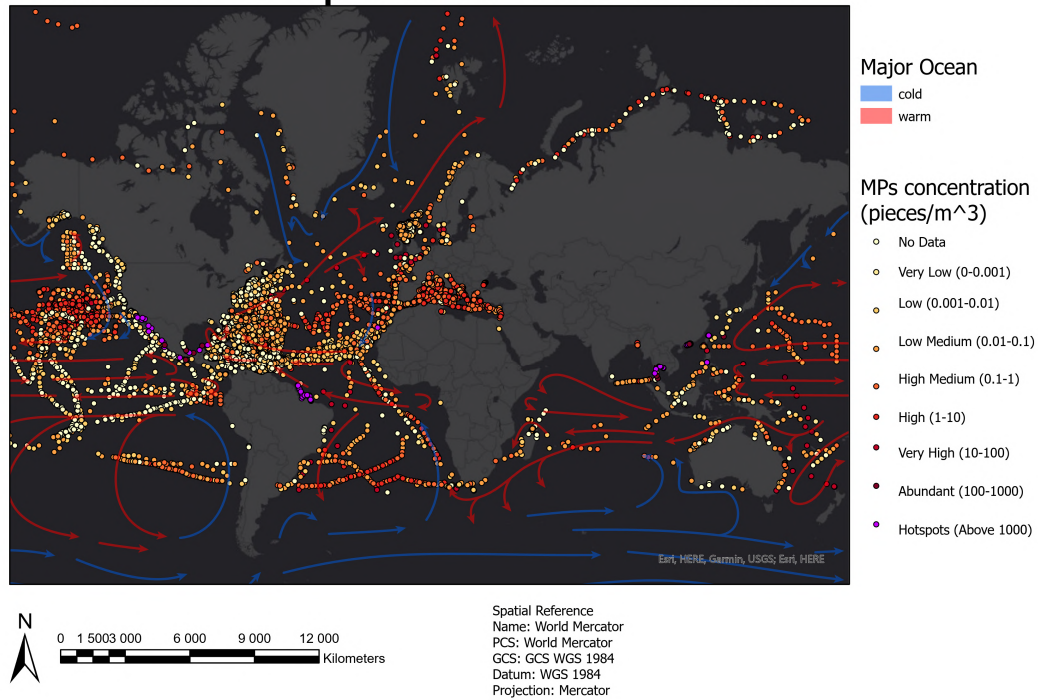


Figure 1.3.1: Global distribution of surface marine microplastics (MPs/m³) with main ocean circulation (blue refers to cold, deeper water and red refers to warm, surface water). Data collected on 30.06.2023 from the marine database [67]).

harmonization are needed for all these steps to address current limitations that often lead to inconsistency in methodologies [72, 75]. More specifically, opportunistic sampling, selection bias, reduced throughput, and expensive are current drawbacks that contribute to designing high-throughput monitoring methods for MPs research [76, 77].

1.3.1 Sampling of microplastics

Because of the omnipresence of MPs in the dynamic marine environment, numerous methods exist to monitor environmental MPs depending on the matrix studied and the questions being answered [78]. Moreover, within each matrix (surface, column, shorelines/beaches or sediment), different methods have different LOD resulting in hard comparison and reproducibility between studies [70]. For this study, the surface water MPs method were further investigated. The major technologies used can be seen in Table 1.3.1 where major limitations consist of the need for a boat, lack of replicates, LOD bound to the mesh size of the net, and/or the amount of water volume collected. The most predominant method used up to today is the manta net for surface water sampling [70, 78, 80]. However, boat dependency is one of the major drawbacks of the manta net methods because it entails further disadvantages like higher cost, limited accessible areas and sampling paths, creating unwanted water turbulence, and a higher risk of contaminating the samples [80, 75]. As mentioned previously, opportunistic sampling is the common ground when it comes to recording MPs distribution in surface

1. INTRODUCTION

Table 1.3.1: Common sampling equipment for surface water MPs research.

| Equipment | Pros | Cons |
|----------------------------------|--|--|
| Niskin bottle | not dependent on a boat, no lower size limit | small volume |
| Manta net/plankton tow/bongo net | large volume and collects only marine litter in cod ends, flowmeter measurements | need a boat, lower size limit (300-500 μm) |
| In-situ pump | over time measurements, no lower size limit | need to attach the pump to a boat |

Source: Brander et al. (2020) [79], GESAMP (2019) [70], Pasquier et al. (2022) [80]

waters [80, 81]. This is due to the frequent towing of sampling equipment from a vessel whenever deemed convenient, resulting in the recording of only one transect, typically following a linear path against the current. If adverse weather conditions suddenly occur, the manta net becomes impractical as stability will be affected, hence, affecting the accurate measurement of the volume-filtered. To increase the sample throughput and render easier and faster sampling methods, other devices need to be implemented to avoid the use of boats while still filtering large volumes of water over wider spatial and temporal scales.

1.3.2 Analysis of microplastics

For MPs identification and characterization, several analytical methods such as spectroscopy or analysis of thermal degradation products are currently used [75].

Visual counting is an observational method on larger MPs to characterise them based on morphologic features like shape and colours. It can also be performed for smaller MPs using a microscope. The chemical composition of the particle can not be confirmed solely with this method.

Pyrolysis-gas chromatography coupled to mass spectrometry (Py-GC-MS) is an analytical technique used to confirm polymer composition in a sample. By thermal degradation, a polymer releases a unique gas that is detected by MS. The LOD of this technique is very low and can detect easily small sizes in the NPs class. However, this method is destroying the particles hence preventing further investigation and characterisation of MPs. When using this method, it is often hard to compare to other studies since the results are reported in weight of MPs whereas other analytical methods often report particle number, shapes, and size.

Nowadays, widely used spectroscopy for MPs analysis are Fourier Transform Infra-Red (FTIR) and Raman. Both of these optical methods look at the vibrations in the polymer's molecule using a light source to measure reflection or transmission from the particles. FTIR can detect particles as small as 10-20 μm while Raman has a LOD of 1 μm [82]. Attenuated Total Reflectance FTIR (ATR-FTIR) is a common method used in the context of surface MPs when LOD is already limited by the mesh size of the net used. Particle selection is needed before spectrum acquisition [76, 83]. Limitations related to common techniques for MPs analysis can be seen in Table 1.3.2.

One thing all of those methods have in common is that they all require either a long processing and analysis time or a combination of different methods which results in time-consuming and expensive methods for processing multiple MPs samples at a once [76, 77]. Hence, there is a need for increasing sample throughput in the analysis of MPs while keeping the accuracy and integrity of the samples. New methods should improve data acquisition time like reducing the spectral acquisition steps for suspected MPs particles in the samples and imple-

1. INTRODUCTION

Table 1.3.2: Common analysis techniques used for microplastic identification and characterisation.

| Techniques | Limitations |
|-----------------|---|
| Visual Counting | Arbitrary, subjective, often leads to misclassification, low accuracy and repeatability |
| Py-GC-MS | destruction of particles, combination with other methods needed |
| ATR-FTIR | prior manual selection bias, interference of water |
| Raman | interference of fluorescence |

Source: Löder and Gerdts (2015) [61], Faltynkova et al. (2021) [76]

menting chemometric and modelling for a more rapid and robust analysis [76, 84]. Indeed, automated analysis has become more and more popular using spectral imaging techniques from focal plane array FTIR (FPA-FTIR) and Raman. Small photomosaics of randomly selected areas of a sample filter are produced where each pixel corresponds to a spectrum. While avoiding the particle selection step and reaching smaller size, these methods are time-consuming and, often enough, only a small part of the samples is analyzed. Decreasing the analysis time and implementing better areal coverage would help towards a more automated analysis for MPs research. Database matching is mostly used to confirm the spectrum of a particle using FTIR spectroscopy [83]. Recently, unsupervised and supervised machine learning (ML) techniques have been used alongside reference spectral databases for creating algorithms that can achieve complex tasks autonomously [83], hence saving time for the researcher and increasing the high throughput of MPs research.

1.3.3 Development of new technologies and methods for microplastic research

Recently, the concept of reproducible analytical pipelines (RAPs) has been used for MPs research to narrow the development of best monitoring practices. Designing a harmonized workflow in combination with testing the technology readiness levels (TRLs) of the new instruments, technologies, and methods that we are trying to implement will help address the lack of reliability and replicability in the field of MPs monitoring. RAPs and TRLs could be used simultaneously on each step of the monitoring workflow to accelerate the adoption of large-scale MPs research (Figure 1.3.2) [85]. Hence, to provide a more rapid RAPs for MPs monitoring and modelling, new automated and autonomous technologies are being developed.

For MPs sampling, ocean monitoring has in the past decades used autonomous vehicles to access remote locations. Unmanned Surface Vehicles (USV) have been used for a wide variety of research applications with different sensors connected to it [86]. Combining an aquatic drone and a manta net technology would be beneficial for MPs research [87, 88]. Recently, an aquatic automated drone [87] and a Portable Catamaran Device (PCD) have been tested in the environment providing promising advantages to MPs sampling campaign.

For MPs analysis, hyperspectral imager (HSI) was first used for remote sensing and ocean monitoring from satellites and airplanes [89] to triage plastics in recycling facilities [42]. This technology has recently been applied to MPs research [76, 62, 90, 91] combined with classifying models to increase the automated analysis

1. INTRODUCTION

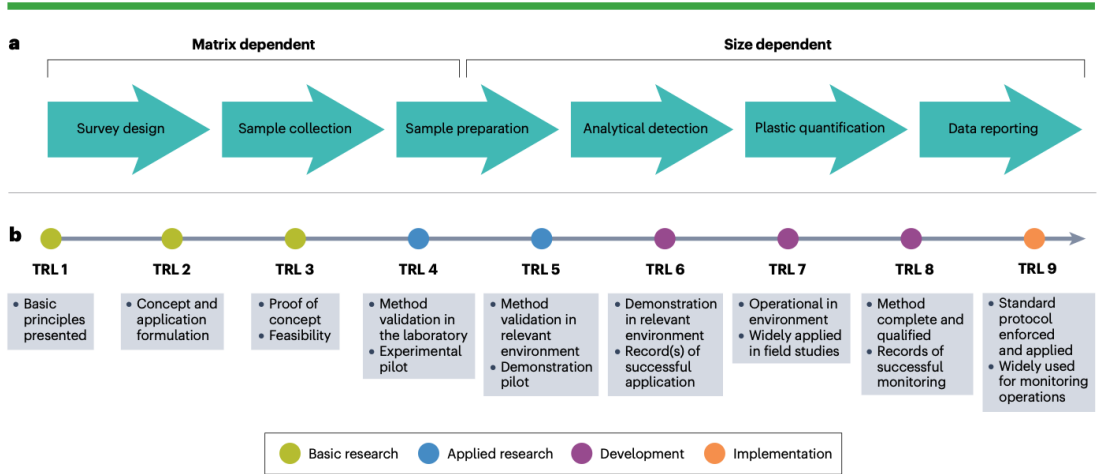


Figure 1.3.2: Reproducible analytical pipelines (RAPs) and technology readiness levels (TRLs) for microplastics (MPs) monitoring. a) shows the workflow for MPs research related to RAPs and b) shows the TRLs that need to be tested for each step in (a) Colors refer where the technology stands in terms of being able to be used for monitoring programs (Taken from Aliani et al. (2023) [85]).

of MPs samples. Briefly, HSI is an instrument composed of an objective lens, a spectrograph that contains an entrance slit, and a two-dimensional detector. A light source is also needed with emission in the visible and IR spectra. The results give a spectrum representative of the different wavelengths of light reflected by a certain plastic polymer, thus, allowing the classification of pixels according to the chemical composition and not just the color [76]. Supervised classification models are used like Soft Independent modelling of class analogies (SIMCA) [84, 92]. These types of models are trained on a specific spectral database containing different polymer types and using Principal Component Analysis (PCA) projections to assign a sample to a specific class or polymer type.

1.4 Scope and objectives

This proof-of-concept study aims to improve the sampling and analysis of MPs by implementing RAPs for long-term, viable, repeatable, and comparable MPs research. For sample collection, a new and autonomous vehicle, PCD, will be used that allows access to remote locations and operations with a spatial and temporal coverage near islands in Runde at the coast of mid-Norway. For sample identification and characterization, HSI will be used to increase area coverage and reduce analysis time and cost. Environmental comparison will be done with an ATR-FTIR, a common and most used method for MPs analysis ($> 300 \mu\text{m}$).

Does facilitating MPs' research through RAPs and TRLs help to increase the representativeness of MPs quantification in the marine environment? To answer that question, a set of objectives were determined:

- Testing the method performance of PCD and HSI for MPs research
- Investigating MPs abundance and morphology with HSI compared to a common analysis technique, ATR-FTIR

1. INTRODUCTION

- Assessing any temporal and spatial differences regarding MPs distribution and environmental factors influence at two different locations in Runde

Disclaimer: Following academic integrity and transparency, I wish to disclose that a manuscript derived from this master thesis has been submitted to OCEANS 2023 [93]. The manuscript shares common raw data but provides distinct interpretations. It is essential to note that certain points in the discussion and conclusion may overlap. However, the intention is to provide complementary perspectives, ensuring a comprehensive exploration of the research topic.

2.1 Study area

The fieldwork was conducted at Runde Island located on the northwestern coast of Norway in the Møre og Romsdal county (Figure 2.1.1) which is part of the Norwegian Sea. Known as the southernmost seabird island on the Norwegian continental

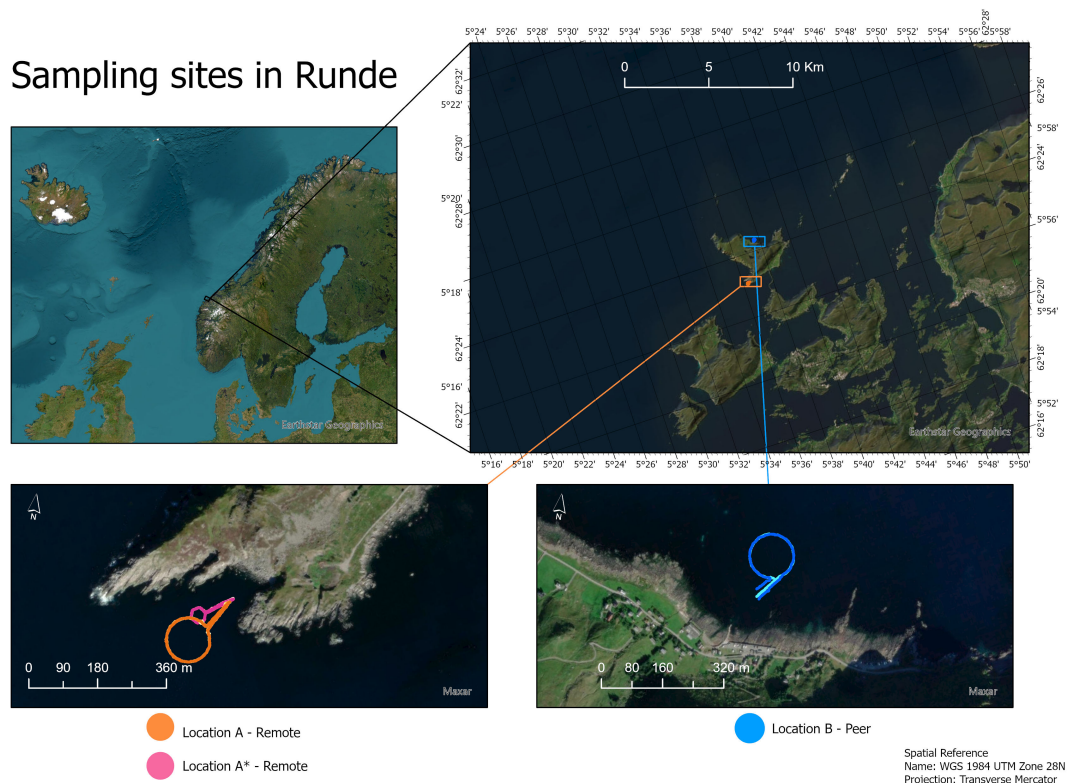


Figure 2.1.1: Sampling sites and the 35 runs at *location A* (680 m) and *location B* (600 m). *location A** emphasizes the shorter path (370 m) used on Day 1 (2022-08-02).

coast as well as the third largest Norwegian bird cliff nesting, Runde became, in 2007, a key site for the National Bird Monitoring Project (SEAPOP). Among the

2. METHODS

230 species that have been documented, several are classified as nationally red-listed species, including notable examples such as the Atlantic puffin *Fratercula arctica* (EN) and the black-legged kittiwake *Rissa tridactyla* (EN) which make their presence valuable for the international significance of this site [94, 95, 96]. The fieldwork was conducted during the breeding period for thousands of seabirds present on the Island. Hence, the conservation area was closed access for the public from May to the end of August. As a result, the sampling locations were selected accordingly.

The island endures a typically oceanic climate with mild winters and cool summers with an annual temperature of 7.6°C and annual precipitation, of over 200 days per year, corresponding to more than a meter (1254 mm) with July 2022 recorded as one of the coldest and wettest summer months in history. Runde is also characterized by its narrow and irregular continental shelf with steep ridges and slope [8], complex hydrography and anomalous bathymetry.

Islands on the coast of Norway are highly impacted by two main currents: the Norwegian Atlantic Current (NAC) and the Norwegian Coastal Current (NCC). Mainly, the NCC originates in the Baltic Sea and mixes with all the freshwater runoffs off the Norwegian coast. The NCC is driven upwards on the continental shelf by the NAC and travels with a faster current speed than the NAC up north bringing with it drifting marine litter. The diverse coastal landscape of Norway, known for its historical heterogeneity, has a well-documented reputation for accumulating marine debris along its islands and beaches [97, 98]. Generally, the NCC is mainly affected by freshwater runoffs, winds, tides, the NAC, and the bottom topography where speed propagates proportionally to water depth. Since winds and tides are factors that govern the NCC, the Key Environmental Variables (KEVs) investigated for this fieldwork were the tide water levels from Runde and wind speed data from Svinøy from mid-July to the end of the field campaign (Figure 2.1.2).

Mid-Norway is governed by the prevailing westerly winds coming from the South and going to the North driven by the low and high pressure of the North Pole during winter and summer respectively. Tide levels follow a semi-diurnal cycle meaning it will have two low tides and two high tides per day. It can also be called mixed tides as the magnitude of the tides is often uneven (Figure 2.1.2). The tide data (water height in meters) was collected from Runde fyr location from the Norwegian Cartography Service Center. The wind data for the fieldwork was from the Svinøy meteorological station located approximately 18 km southwest of the sampling site at *location A*. Hourly wind speed data were collected from the Norwegian Weather Service Center.

2.1.1 Sampling locations

The fieldwork was conducted at two different sampling locations from 02.08.22 to 06.08.22 (Figure 2.1.1). Samples were collected every day throughout the day ranging from eight to ten samples per day. The sea state observed during fieldwork was from 0 (no waves) to 4 (1.4-1.6 meters waves) on Beaufort scale [88].

2. METHODS

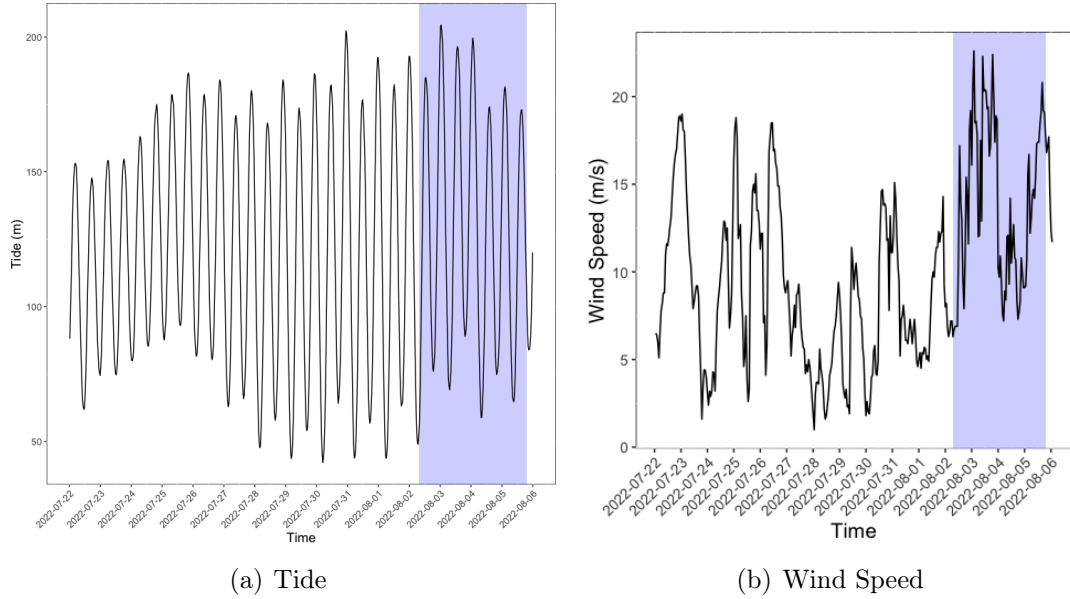


Figure 2.1.2: Fieldwork window in blue compared to tide and wind data two weeks before fieldwork. a) Tide data (m) per 20 min from Runde fyr and b) Wind data (m/s) per hour from Svinøy station (SN59800)

Location A was the primary and exposed location. It is situated on the South-West side of the island and hence very impacted by the currents and predominant south-westerly winds. The surrounding areas are cliffs and a protected conservation area for birds. Hence, confounding factors related to human disturbances are judged to be relatively low.

Location B was on the island on the northeast side and sheltered because it could benefit from protection against strong currents and westerly winds. The deployment of the robot was done from the pier next to the local campground near human habitation.

2.2 Fieldwork

2.2.1 Sampling services and design

Sidenote: In this work, the words runs, transects, and samples are used as synonyms all referring to the "replicates" of the field campaign.

Portable Catamaran Drones (PCD) were used during the four days of fieldwork in Runde, Norway. Three units were brought by car to Runde Environmental Center. The units were dismantled before transport and secured with bungee straps. Before fieldwork, the robots were assembled. Additionally, the two flowmeters (Hydro-Bios, 438 110) and two nets (Hydro-Bios) with dimensions length, width, height, and mesh size (respectively, 200 cm, 30 cm, 15 cm, 300 μm), eight 18V 5Ah batteries (BL1850B, Makita Corporation, Japan), tablet for QGround control App (4.1.1), and six cod-ends (300 μm mesh size) with their glass jar container and

2. METHODS

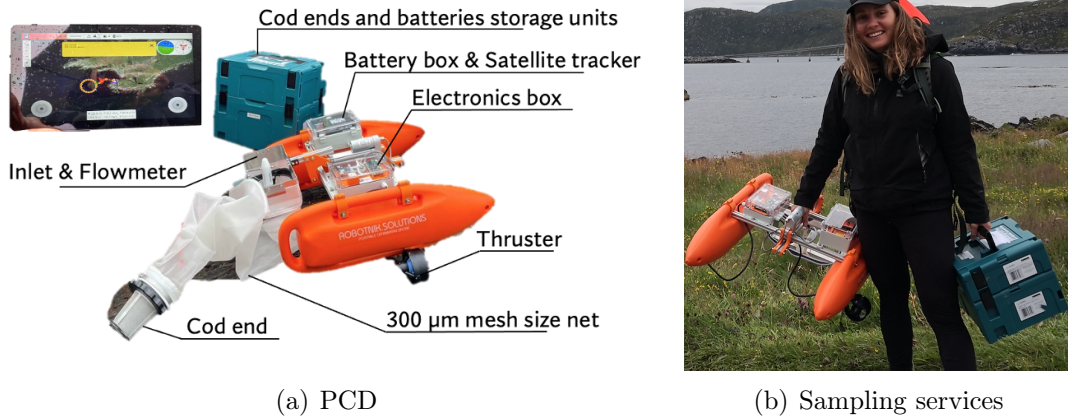


Figure 2.2.1: Overview of the robot’s components and the equipment needed for fieldwork: a) displays all the principal components of the Portable Catamaran Drone (PCD) and equipment and b) shows a researcher carrying all the equipment provided by the sampling services to the fieldwork site

their silicon lid. All of this equipment combined constitutes the sampling services provided by PCD (see Figure 2.2.1). For easy sample management, custom-made cod-ends and batteries can be changed rapidly after each run. For better control over the intake of water, the inlet was designed to be lifted and/or lowered on command. Zolich et al. (2022)[88] report further details about the different components of the robots, other necessary equipment for sampling, and specifics about the manufacture and the control electronics design.

Before sampling, automated paths were prepared an open-source software for drone deployment, Mission Planner (1.3.77), and sent to the robot used through LTE connection. By selecting certain amounts of waypoints, a main circular path was created to counter the effect of currents. This main path is located some meters away from the deployment site to allow the addition of two key features in the automated path: a launch (or return) position as well as a command (Set Relay) telling the robot to lower (or lift) the inlet in (or out) of the water (see Tablet in Figure 2.2.1 and path shape in Figure 2.1.1). When launching the robot in the water, a researcher needs to drive the robot manually with the tablet to avoid the vehicle getting stuck in waves or kelp.

Three different transect lengths were prepared (370 m, 680 m, 600 m), but all had a similar shape (see Figure 2.1.1). At *location A*, on the first day of fieldwork (2022-08-02), we tested the performance robot with a shorter path (370 m) that we increased (680 m) on the consecutive days at that location since the vehicle was functioning accordingly. Then, at *location B*, a similar path length (600 m) was planned.

On average, the robot was trawling for 20 min per sample before it could be recovered. We allowed approximately 20-30 min between samples for replacement of cod-ends and batteries as well as recording the flow meter readings. Moreover, the used cod-ends were stored immediately in a glass jar with a silicon or alu-

2. METHODS

minium lid to prevent any atmospheric contamination. Additionally, we tested the deployment of two units at the same time at *location B* where the robots were launched 5 min apart from each other following the same path.

2.2.2 Sample processing for transport and storage in Runde

In Runde Miljøsender, laboratory facilities were used in the evenings to process the samples from the field to store them properly for transport and storage. The cod-ends needed to be rinsed the same day of sampling to prevent the organic matter from drying so it could be removed more easily. Hence, the stainless still cod-ends were rinsed thoroughly with ultrapure water in their glass container first. The cod-ends are flipped upside down in a plastic funnel in a 1 Liter beaker. Samples were then vacuum filtered on one (or more) 100 μm stainless steel filter depending on the amount of organic matter in the sample. Filters were stored in 20 mL glass vials in 70 % Ethanol for transport to NTNU for further sample preparation and analysis.

2.3 Quality assurance/quality control protocol

When implementing a new and more repeatable method for MPs collection and characterization, there is a need for accurate measurements and trust in the output results of MPs research. A thorough setup for field and laboratory QA/QC has to be in place to minimize contamination of the samples. However, even if all precautions are taken (i.e. avoid plastic equipment, wear cotton clothes, clean surfaces, and clean and cover glasswares), the ubiquity of MPs is extremely variable. Hence, the need for blanks at every step of the sample processing is crucial. Data from these blanks should help improve accuracy, and repeatability, and account for variability by correcting for sample contamination.

QA protocol was followed taking all precautions possible. Before the fieldwork, in Trondheim, scintillation glass vials, for sample storage, were cleaned and rinsed with ultrapure water and ethanol 75 % three times before being oven dry at 90°C for 4 h. Moreover, during all laboratory processing steps, all surfaces were cleaned with ultrapure water and/or ethanol. All glassware was rinsed with ultrapure water. Furthermore, cotton lab coats and clothes were used at all times while handling samples in the laboratory and any plastic equipment was avoided when possible. Aluminium is used to cover glassware and instruments when not in use to prevent contamination and is carefully removed when adding chemicals but quickly put back on.

QC is a crucial step for sample processing. First, a total of five field blanks were implemented per day and per location where one glass fiber filter (Whatman GF/F, 47 mm diameter, pore size 0.7 μm , WHA1825047) was left exposed when changing the cod-ends in-between sample collection and stored for analysis in a glass petri dish with tape to prevent any contamination during transport and storage. The field blanks were not processed further alongside the samples to isolate contamination from the field.

Analytical blanks were introduced at two different steps in sample processing. In the laboratory in Runde, eight blanks (B1a,b - B4a,b; see Table 2.4.1), two

2. METHODS

per day, were made following the same procedure as Section 2.2.2, but using a clean cod-end. In the laboratory at NTNU, another seven analytical blanks (A-G, see Figure 2.4.1) were added in all seven batches of sample processing (see Section 2.4.2). In total, 15 analytical blanks are carried throughout sample processing and stored with the samples for analysis.

Finally, to assess sample processing recovery rates, artificial samples were intentionally spiked with known MPs. The preparation of spiked samples was carried out by a researcher independent from the MPs analysis, ensuring impartiality. These spiked samples incorporated fragments or pre-production pellets (approximately 3 mm Feret diameter) and cryo-milled microplastics (500-1500 μm Feret diameter), adding them in known quantities to a vial containing ultrapure water, algae culture, and dried leaves. Further details can be seen in Faltynkova et al. (2023) [99]. The spiked samples included combinations of six polymer types: PE, PP, PET, PS, Nylon, and PLA-based bioplastic. Notably, four of these polymer types can be identified through NIR-HSI analysis, while Nylon and bioplastic were included to assess potential false positives. Three spiked samples, prepared and analyzed in parallel with all other samples, served to validate the recovery rates during the evaluation process.

2.4 Sample preparation in the laboratory at NTNU

Sample preparation and processing was done at NTNU. Optimization of the methods for the chemical digestion of the organic matter was done in the laboratory in the Fall of 2022 according to NOAA Marine Debris program recommendations from 2015 [74]. Tests were performed on dummy samples only to increase the high-throughput efficiency of processing multiple samples at a time without damaging any samples. Therefore, the protocol mentioned below was adapted from Liu et al. (2019) [100] to extract the MPs from their ethanol and organic matter.

2.4.1 Soaking in soap for sample storage

To release the organic matter from the filters more easily for subsequent oxidation processes, the ethanol was evaporated from the vials (samples, blanks, and spiked samples) over seven hours for three days at 50-70°C on a heat plate. Lids were removed from the vials and replaced by an aluminium sheet with holes. Vials were carefully monitored to make sure the organic matter did not dry completely in the vial and on the stainless-steel filters. Since the spiked samples were made with ultrapure water, the evaporation took longer in the vials, so, to increase the heat surface-area ratio, we transferred them to glass petri dishes. To be able to efficiently remove all matter from the filters, we needed to soak the samples in a Sodium Dodecyl Sulfate (SDS, 5 %) soap solution. In a 1 L beaker, 50 g of SDS (Sigma-Aldrich, 75746) was dissolved in 800 mL of filtered ultrapure water while mixing, with a stir bar, on a heat plate at 30°C for 30 min. The solution was then slowly poured into a 1L volumetric flask to avoid bubble formation. The volumetric flask was filled up to the line with filtered ultrapure water. The solution was then vacuum filtered over a glass fiber filter (Whatman GF/F, 47 mm diameter, pore size 0.7 μm , WHA1825047) with an ethanol trap to trap bubbles. Once the ethanol

2. METHODS

was almost all evaporated from the vials or Petri dishes, SDS aliquots were added to fill the vials or Petri dishes approximately halfway. On month and a half later, 20 mL of 5 % SDS solution was added to fill the vials. All the vials and Petri dishes were then transferred to an incubator-shaker (IKA KS 4000 i control) for 24 h at 75 rpm and 50°C. After 24 h of incubation, spiked samples were thoroughly washed and rinsed from their Petri dishes back into their original vials. All vials were sonicated for five to ten minutes at room temperature. Vacuum filtration with an ethanol trap over new 100 μm stainless steel filters where the old filters were rinsed and cleaned. The organic matter and, potential MPs, were stored in their vials with filtered ultrapure water.

2.4.2 Fenton reaction

Blanks, samples, and spiked samples were split into seven different batches (Table 2.4.1).

Table 2.4.1: Samples and spiked samples distribution for the different batch processes in the laboratory. Some batches contain fewer samples because some samples were divided into separate vials because of a higher amount of organic matter in them. Analytical blanks from the laboratories in Runde and NTNU (B1a,b - B4a,b; A-G) and artificial spiked samples (SS1-SS3)

| Batch | Samples | Blanks and Spiked Samples |
|-------|---------|---------------------------|
| 1 | 1-6 | B1a, A, SS1 |
| 2 | 7-11 | B1b, B2a, B |
| 3 | 12-14 | B2b, C |
| 4 | 15-20 | B3a, D, SS2 |
| 5 | 21-25 | B3b, E |
| 6 | 26-29 | B4a, F |
| 7 | 30-35 | B4b, G, SS3 |

The oxidation of the organic matter was done using Fenton reagent (0.05 M), hydrogen peroxide (35 % H_2O_2 , Sigma-Aldrich, 1.08600), and sodium hydroxide (0.1 M NaOH solution, Sigma-Aldrich, S5881) 1 L of Fenton reagent was prepared by mixing 30 g of Iron(II) sulfate heptahydrate ($\text{FeSO}_4 \cdot 7\text{H}_2\text{O}$, Sigma-Aldrich, F7002), 6 mL of sulfuric acid (95-97 % H_2SO_4 , Sigma-Aldrich, 1.00731), and 1 L of ultrapure water. For all batches, except for Batch 1, all vials were rinsed and transferred to a 1 L beaker. The amount of ultrapure water used for cleaning was sure to not reach a total volume of 80 mL. Then, 60mL of H_2O_2 and 25 mL of 0.1 M NaOH solution. Manual mixing was applied after each chemical addition by swirling the beaker. For the Fenton reagent addition and to reach a final 10 % H_2O_2 concentration, 50 mL was added over 1 h, adding 10 mL aliquot every 10 min and ensuring good mixing between each addition while carefully monitoring the temperature of the reaction. Indeed, the Fenton reaction can be quite active and create a lot of bubbles as heat is released off [74]. Temperature was monitored with an air gun to prevent contamination, which would have been introduced using a thermometer inside the beakers, and for more efficient monitoring of multiple beakers at a time. When the reaction was warmer than 30°C, the beakers were

2. METHODS

placed in an ice bath to cool off to at least 20°C. After all aliquots of Fenton reagent were completed, monitoring of the reactions was carefully done for the following two hours or longer, at least until all reactions had stopped (no more bubbling) and all reactions were lower than 25°C for more than 30 min. Beakers were left overnight to ensure the success of the reactions. For batch 1, the final H₂O₂ concentration was 5 %. The chemicals added were: 100 mL ultrapure water, 32.5 mL of 0.1 M NaOH, and 40 mL of 35 % H₂O₂. This was corrected in the future batches to reach a higher concentration of H₂O₂ for a more efficient oxidation. No differences were observed since the low amount of organic matter in batch 1 did not require harsher oxidation conditions.

2.4.3 Filtration

After an overnight Fenton reaction, all beakers were vacuum filtered on one (or more) glass fiber filter (Whatman GF/F, 47 mm diameter, pore size 0.7 µm, WHA1825047) and stored in clean glass Petri dishes for air drying without the risk of atmospheric contamination. Multiple filters were used in the case where organic matter was too high to prevent overlap of particles for imaging. Dried samples were stored for further analysis.

2.5 Microplastics analysis and characterization

For this research, MPs were recorded with a lower limit of 300 µm due to the sampling net mesh size and an upper limit of 5000 µm. Some particles were found outside those limits, they were not discarded for analysis, but they were analyzed separately when the size of the particles was investigated.

2.5.1 HSI analysis

A HSI was used to image all the filters from the fieldwork which took approximately 5 h. The model of HSI is HYSPEX SWIR 320 HI (Norsk Elektro Optikk) with the Hypspx software(V.3.5). Each filter was laid in the field of view (FOV) of the HSI camera where it could scan and collect near-infrared (NIR) spectra in diffuse reflectance mode. The spectral range was 962-2493 nm (10395-4011 cm⁻¹) and a spectral resolution of 6 nm (see Faltynkova and Wagner (2023) [84] for further details). Two Hypspx halogen lamps are used for an artificial light source. A spectral reflectance standard was taken for the light source so that all spectra could be normalized, resulting in relative reflectance. By stitching lines of single pixels together while scanning the filter horizontally and sampling multiple wavelengths at the same time, data acquisition was rapid and efficient.

The FOV and corresponding image of this system (16 x 53 mm, 320 x 1000 pixels) correspond to only a third of the height of the filter used (47 mm in diameter). To cover the entire filter, 3 line scans needed to be taken for each filter. Hence, all samples would have at least 3 HSI images, if they had only one filter per sample. Using ENVI software (2023, L3Harris Geospatial Solutions, Inc.), the 3 images related to the 3 different positions on each filter were stitched together to create a photomosaic (960 x 1000 pixels x 256 wavelengths). These photomosaics were processed following the method developed by Faltynkova and Wagner (2023) [84].

2. METHODS

In summary, MPs are detected by, first, using a SIMCA model for the classification of pixels. This model is open source and can be accessed on GitHub. Secondly, ImageJ (V. 1.53t) [101] was used for counting and characterizing particles by size (see Appendix 5 for batch processing code).

Data processing was conducted using R (V. 4.3.0) on a local computing cluster [99, 102]. Following Faltynkova and Wagner (2023) [84] recommendations, the LOD for MPs size was set at 300 μm and the limit of quantification (LOQ) was set at 500 μm . The model could only identify four polymer types: PE, PP, PS, and PET.

2.5.2 Microscope and FTIR analysis

For method comparison, hand picking, microscope image capture, and FTIR analysis of suspected MPs particles were performed [103]. All filters were thoroughly (scanning from left to right) inspected for suspected MPs particles using a stereomicroscope with a connected camera (Zeiss Axis Zoo.V16 fluorescence microscope). An image of each particle was saved with the longest distance (Feret diameter, μm) measured. Visual characterization of particles' colour and shape was done following Lusher et al. (2020) [104] framework. Hand-picked suspected MPs particles were collected in 6x4 well plates for storage and transport to the FTIR instrument [103]. Each suspected particle's transmittance spectra were measured using an FTIR (Bruker Alpha Platinum ATR-FTIR). The spectral range was 4000-400 cm^{-1} and the spectral resolution was 4 cm^{-1} .

Spectral pre-processing was done using Microsoft Excel for Mac Version 16.73 (23051401), RStudio version 2023.03.0+386, and R version 4.2.1 The spectra files were exported and converted for OpenSpecy library search [105]. In OpenSpecy [105], the spectra were smoothed (polynomial of 3) and baseline corrected (polynomial of 8). Spectral matches with a Pearson's R correlation > 0.7 were assigned the polymer type given by the match. Moreover, if the spectrum was hard to identify, the visual microscopic images were used as well as investigating specific peaks in the spectral range in OpenSpecy [105]. Particles were excluded from analysis if their library search was linked to a specific contamination source or resulted in a non-synthetic material, but natural material like natural fibers from clothes, cellulose, or algae.

Overall, all MPs metadata (samples, blanks, and spiked samples) can be seen in an Excel file (see Appendix 5).

2.6 Polyvinyl chloride spectral database implementation

Providing that the current SIMCA model only accounts for four polymers (PE, PP, PS, PET), the addition of PVC was investigated. Only a small amount (11 in total) of consumer PVC products (9) and environmental PVC plastics (2) were added to the spectral database. The consumer products were either used or bought new, including water tube from a sport water bag, transparent food wrap from the UK and USA, a sport dry bag, a pipe, a material found in showers.

2. METHODS

The environmental plastics are a grey pipe and a big triangular piece found in beaches clean-up plastic in Norway. Following Faltynkova and Wagner (2023) [84] workflow, PVC products were first confirmed using the FTIR instrument with a similar method as in Section 2.5.2, but confirming the polymer with the Opus Library from the instrument. Then, HSI photomosaic were acquired following the same procedure as in Section 2.5.1. In ENVI software, regions of interest (ROI), i.e. plastics, were selected on the HSI image. The ROI were 12 blocks of 2x2 pixels, resulting in 48 spectra for one plastic. Each 4 pixels within a block were average, reducing the number of spectra per particle to 12. Hence, 132 spectra were acquired for PVC. Validation and training of the SIMCA with PVC was not part of the core of this thesis. Further spectra acquisition of PVC is needed before implementing it in the model to ensure specificity.

2.7 Spatial and statistical analysis

For spatial analysis, all maps were made in ArcGIS Pro Version 3.0.1. For the global distribution of MPs, Mercator world projection was used and the point layer corresponds to GPS coordinates of MPs concentration taken from the NOAA marine database (data accessed 30.06.2023) [67]. The polygon layer related to global ocean circulation is taken from NOAA Maps. For local maps related to fieldwork, maps were created using GPS coordinates of each 35 runs throughout the field campaign with Transverse Mercator projection and Datum WGS 1984 UTM Zone 28N.

For statistical analysis, metadata were collected in Excel to produce CSV file for further analysis in RStudio and R. Statistical tests below were done using R package *stats* version 4.2.1 and R package *rstatix* version 0.7.2. A Shapiro-Wilk test was performed to assess the normal distribution of the concentrations, MPs size, and KEVs. Due to a rejection of the null hypothesis, non-parametric tests were used. A Wilcoxon Signed rank test (or Mann-Whitney U test) was used to compare differences between volume measurements. Kruskal-Wallis test was used to compare numerical variables (concentrations and size) and categorical variables (Instrument, Location, and Dates). Multiple comparison between dates was further assessed by a Dunn test. We decided to report medians and means in the results section for a simpler and more accurate comparison with other literature on MPs concentrations in surface waters. Correlations were investigated between MPs concentrations and KEVs using fitting linear models.

3.1 Methods performance

Combining the PCD and HSI can improve the performance of MPs research. RAPs are needed in MPs research [85]. Combining both methods and assessing their performance relative to common practices in the field and laboratory is helping investigate TRLs for both new technologies in MPs research.

3.1.1 Portable Catamaran Device

Over the 35 samples collected in Runde at two different locations (A and B), 15.2 km of surface water were sampled over 7 hours and 15 minutes, spanning four days from August 2nd to August 5th, 2022. The average distance travelled per sample was $460 \text{ m} \pm 200 \text{ m}$ with an average sampling time of $13 \pm 6 \text{ min}$ which resulted in an overall speed of $0.58 \pm 0.05 \text{ m/s}$ (1 knot) (Table C.1 in Appendix).

The sampling worked efficiently and smoothly for 77% (27/35) of all runs. One person could easily carry all the materials needed. This included two boxes containing batteries and sample containers, and the robot. Hence, the fieldwork was easily doable with two researchers (one for controlling the USV via a tablet and the other for physically putting the robot in the water) and one expert user assisting remotely. The two sampling locations were easy to reach by foot or car without the assistance of a boat. In general, the PCD demonstrated promising and successful performance, offering several advantages. This includes lowering of the net, launching of two PCD units at approximately the same time, and the stability of PCD in harsh weather with a Beaufort scale 4 (wave height of 1.2 m).

Technical difficulties were encountered during the fieldwork. Physical difficulties involved kelp being stuck in the propellers while driving the vehicle manually away from the launching site near the rocks. Navigation system problems were encountered, encompassing challenges such as compass malfunction, communication loss with the vehicle, and overheating in the battery compartment causing condensation in the electronic box on the vehicle. All issues could be resolved on-site while communicating with the remote expert user who could track and control the

3. RESULTS

vehicles via the mobile network. Although these events were successfully resolved, some still resulted in loss of data from the GPS logs and diverging paths from the initially planned path. These errors are highlighted respectively in green and yellow (Figure 3.1.1, Table C.1 in the Appendices).

Differences in technical difficulties were observed at different locations. Kelp entanglement was more prone to happen at location A where one propeller would stop working (runs 11, 24, 25). At location B, launching the vehicle was relatively easy from the pier. However, the presence of steel cables in the water has been suggested to affect the compass which needed the assistance of the remote engineer for re-calibration (runs 16, 31). GPS logs were damaged or misplaced for runs #7 and #12 due to potential file system errors. Moreover, for transect #20, the system only recorded a very short sampling time resulting in wrong distance, duration, and power usage compared to the other normal runs (Table C.1 in the Appendices). Overall, less than 25 % of the runs needed assistance (physically or electronically) and all errors were solved either directly on-site or with the help of the engineer who could control the robot remotely.

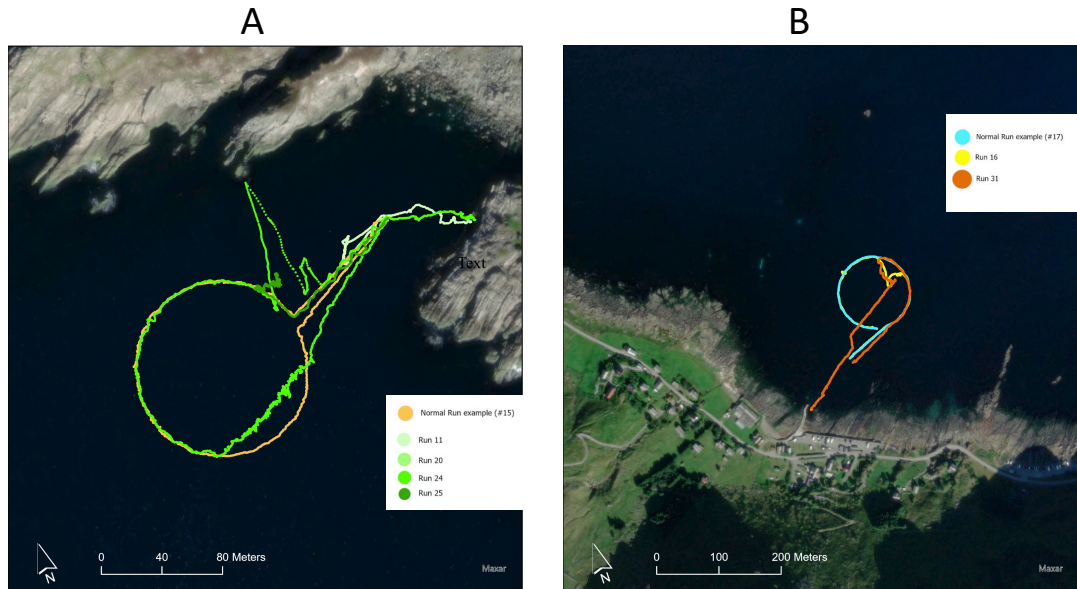


Figure 3.1.1: Technical difficulties encountered during the fieldwork for specific transects at *locations A and B*. A normal trajectory is shown in each location as a reference. Ranges of yellow colors correspond to system issues whereas green colors correspond to physical issues

Sample volume is the most important factor in the context of MPs research. The volume of water for each transect was recorded using a flowmeter and GPS data. A total of 655.1 m³ (18.6 ± 7 m³ per run), calculated with GPS, or 503.9 m³ (14.4 ± 6 m³ per run), calculated with the flowmeter, of seawater was filtered during the field campaign. For some transects, the flowmeter was not installed on the robot in use (#3 - 10) or it got loose from the frame and was then pushed to the side, unable to measure the right volume of water going through the net. If this was the case (#3-10, #12, #21, #26-27, #34), an average of the volumes calculated for a specific day at one of the locations was used for calculating MPs concentration. For further volume comparisons and MPs findings discussed below,

3. RESULTS

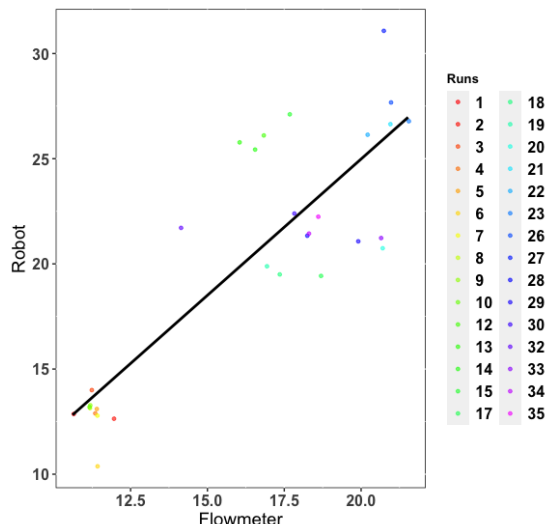


Figure 3.1.2: Comparison of volume measurements taken from the flowmeter and the robot overall completed runs. The positively correlated linear regression trendline shows a significant difference between the measurements. Scatter-coloured dots correspond to all the completed runs used in this result section.

runs 11, 16, 24, 25, and 31 were excluded because they did not finish the full planned path due to errors mentioned in Figure 3.1.1. Moreover, the volumes for each completed run from the flowmeter were found to be significantly lower as compared with the GPS-based volume calculation (paired t-test, $p < 0.001$, Table B.1 in the Appendices, Figure 3.1.2).

Overall, all three robot units operated similarly, but further investigations are needed towards volume measurement differences between flowmeter and the robot. Considering our data and previous studies for MPs sampling with a manta net, we decided to use the flowmeter data for MPs concentration.

3.1.2 HyperSpectral Imager

By evaluating the performance of HSI method to the conventional FTIR method in MPs analysis, substantial time reduction and similarities in MPs recovery were shown.

The analysis time was five times faster when using the HSI method. Indeed, while FTIR requires approximately 60 h for visual inspection and selection of particles and 70 more hours for analysis and open source library confirmation of polymer type, HSI only needs a total of 5 h for analysis of filters and 20 more hours for running of the SIMCA model through a local cluster with image analysis. Overall, MPs analysis, which corresponds to a crucial yet laborious step in MPs research, took 130 h with microscopy and FTIR compared to 25 h with HSI.

Validation of HSI compared to FTIR was investigated using three spiked samples (artificial seawater samples with PE, PP, PS, PET, PLA, and Nylon 6) and comparing their recovery rates (combining all three spiked samples together) between the two methods. By comparing the sensitivity between instruments, HSI had a

3. RESULTS

recovery of 59 ± 9 % and FTIR had a recovery of 60 ± 10 % regarding PE, PP, PET, and PS. More specifically, the rates were relatively similar for PET (35 % for both) and PS (64 % for both) whereas the PE rate was higher for HSI (75 % > 65 %) and the PP rate was higher for FTIR (66 % > 54 %). This was investigated thoroughly by another colleague in the project [99]. In summary, ground truth values were significantly different compared to the two instruments showing that both are underestimating the amount of MPs in a sample. This can be explained by various factors including potential loss of MPs during laboratory processing steps and/or during analysis steps recorded by FTIR. When comparing results between the two methods, false negatives can explain the underestimation of MPs as both methods have limitations. Nonetheless, it was found that both results were comparable in number and non-significant where HSI missed 7 PP particles and FTIR missed 6 PE and PS particles. Moreover, false positives can also occur during analysis. Both methods encountered false positives. FTIR assigned copolyester to particles that were PLA polymers in SS3 whereas HSI detected more PE particles than the true value of the spiked samples (Figure 3.1.3) for two out of three sample recovery tests. Moreover, HSI detection can have limitations regarding thinner particles resulting in several patches of the same particle in the false color image as seen in Figure 3.1.3. This was corrected in the total number of PET particles detected for the calculation of the recovery rates. Overall, the methods were cross-referenced with artificial seawater spiked samples containing known amounts of MPs polymer types which helped us assess the similar patterns between the two methods to further compare the environmental results from Runde.

3.1.3 Improving HSI: PVC implementation in SIMCA model

PVC was added to the spectral database associated with the SIMCA model to prove that, although our HSI method is limited to four different polymers (PP, PE, PET, PS), we can still easily add new polymers to the training data. By inspecting the scores plots of each PCA, some subgrouping and general trends can be observed. For PVC, weathered plastics from the ocean are clustered towards one end of the second principal component (PC) axis whereas consumer products are spread along the PC1 axis (Figure 3.4(a)). The number of consumer products was nine compared to three for weathered marine plastics. The larger variety of the PVC consumer product spectral database could explain the more pronounced dispersion along the PC1 axis. Moreover, the different applications PVC is used for and different chemical additives can explain this trend in the spectra. When we looked at the scores plot including all polymers, the difference can be seen where more aromatic polymers (PS and PET) are situated on one end of the PC2 axis whereas the polymers with increasing non-aromatic covalent bond energy (PVC, PP, PE) are skewed on the other side towards PC1 axis (Figure 3.4(b), Table 1.2.2). The considerable overlap between the types of plastic products proves that all initial polymer types (PE, PET, PP, PS) can still be classified in the model correctly [84] which can be hypothesized if PVC would be added in the SIMCA model. Overall, a more extensive dataset of hyperspectral fingerprints for PVC is needed to fully implement it into the model and confidently assign it to environmental data as well as the need to test cross and external validation for checking the model authenticity.

3. RESULTS

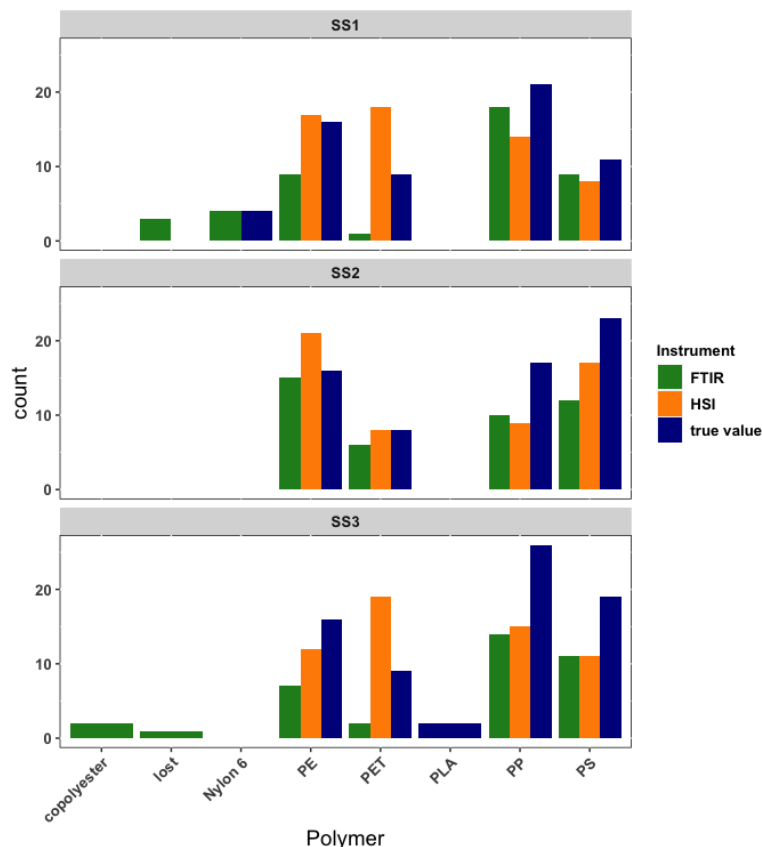


Figure 3.1.3: Comparison of the two methods, FTIR (green) and HSI (orange), using three artificial seawater spiked samples (SS1, SS2, SS3) as the true value (blue). Polymers, in known amounts from the spiked samples, are polyethylene (PE), polypropylene (PP), polystyrene (PS), polyethylene terephthalate (PET), polylactic acid (PLA). Count refers to the sum of plastic particles for each polymer in the spiked samples measured with the different instruments and compared to the true value.

3.2 MPs findings: environmental comparison of HSI with microscopy and ATR-FTIR

3.2.1 Quality Assurance and Quality Control

MPs ubiquity requires a contamination protocol using field and analytical blanks throughout the sample processing steps. Field blanks were introduced during fieldwork when the samples were exposed to air to rule out a potential atmospheric contamination whereas analytical blanks were introduced during the different laboratory steps and carried through the procedure until the analysis. A thorough QA/QC protocol was followed throughout the study.

Blank correction was considered using LOD/LOQ method from Dawson et al. [106]. Through examination of the blanks, due to the low density of MPs in the sample, and almost no MPs detected in the blanks (one PP for FTIR results and none for HSI), the data was not corrected using the blanks. However, we identified a specific contamination source by matching FTIR spectra of MPs in the samples to pieces of the sampling equipment. Indeed, a clear indication of sampling contamination was identified. POM particles were identified in several samples (33

3. RESULTS

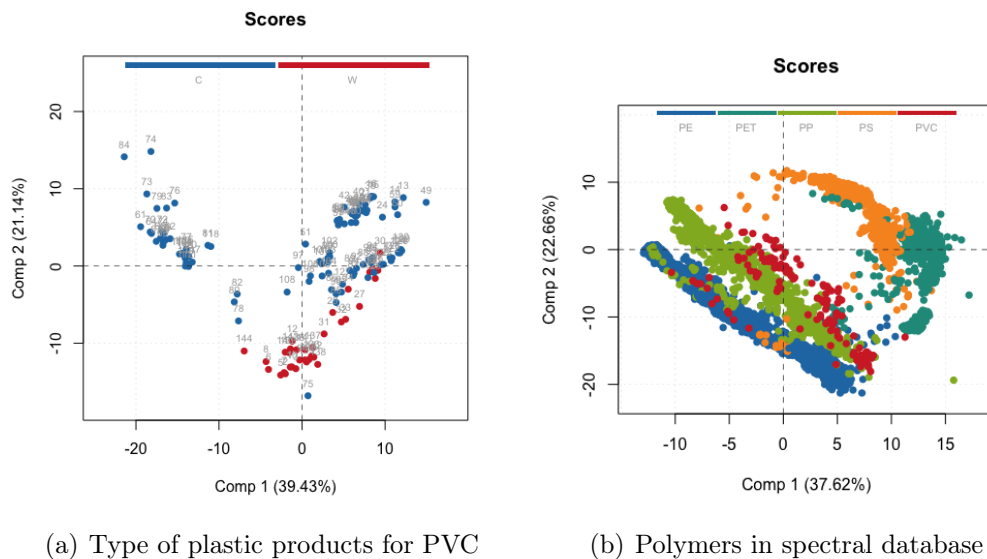


Figure 3.1.4: Incorporating polyvinyl chloride (PVC) in the spectral database. a) Principal component analysis (PCA) scores plot comparing PVC plastics origin: C for consumer products and W for marine plastics and b) PCA scores plot comparing the different polymers from the spectral database with PVC

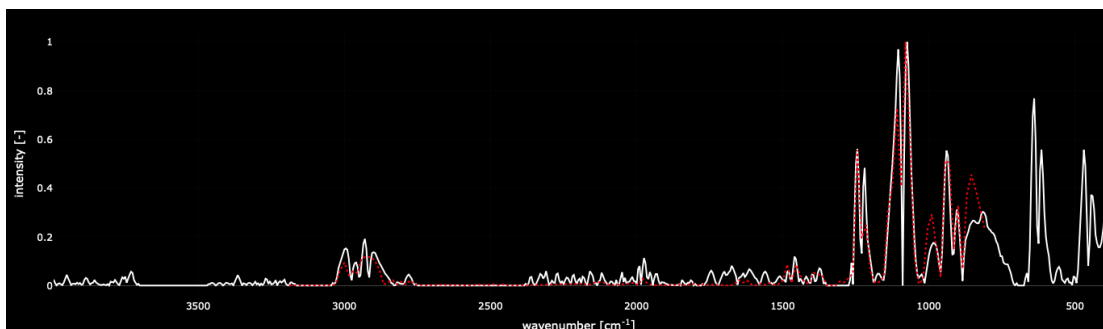
particles) and blanks (4 particles), (see Appendix 5). More specifically, it is found in the analytical blanks created in Runde where a cod end was rinsed with distilled water. Since the cod end is screwed on using a plastic 3D-printed POM ring, we assumed that pieces of the plastic can be shed which end up in the cod end with the sample. Two ATR-FTIR analyses of two different fragments of the ring confirmed POM and matched the spectra of the POM particles in OpenSpecy database [105] (Figure 3.2.1). Their similar physical characteristics correspond to shredded fragments or fibers often entangled together and associated with a grey colour potentially due to the oxidation treatment (Figure 3.1(c)). Moreover, POM is known to have a higher density than seawater (1.41 g/cm^3). Therefore, it is an unlikely polymer to be found in surface water samples which is why these plastics were excluded from further analysis. Overall, this one is the only known and confirmed contamination that was captured by the FTIR results and not the HSI because the HSI can't detect POM polymers in the SIMCA model yet. Characterization of the colours for each suspected particle was done (see Figure C.2 in the Appendices) and can help identify equipment contamination.

3.2.2 Abundance and Morphology of MPs: investigation of technical and spatial differences

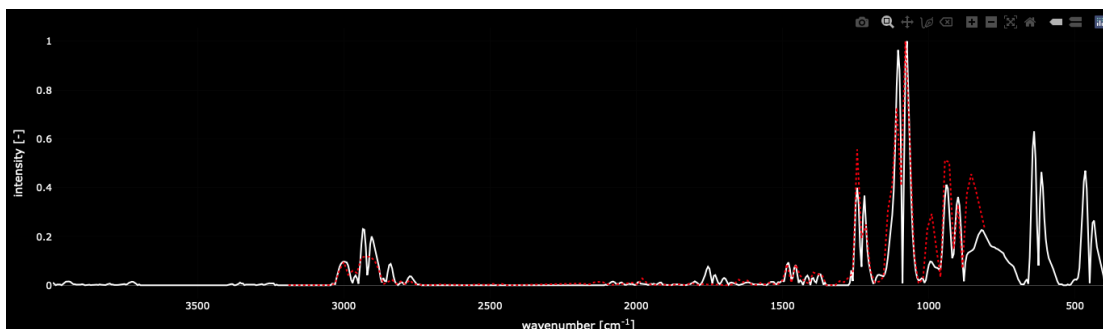
The total abundance of detected MPs was 46 particles for FTIR and 48 for HSI. We normalized this abundance by the volume of each transect to calculate the concentration of MPs at Runde. Transects with unfinished original planned path (#11, #16, #24, #25, #31, see Figure 3.1.1) were excluded. Concentrations per transect throughout the field campaign were highly variable (Figure 3.2.2).

For FTIR, the mean concentration was $0.09 \pm 0.1 \text{ MPs/m}^3$ and the median

3. RESULTS



(a) POM particle



(b) POM from the ring on the net



(c) Example of POM particle found

Figure 3.2.1: Polyoxymethylene (POM) spectral fingerprint from sample compared to a known contamination source using OpenSpecy [105]. a) Showing one of the spectral signatures of a fiber found in a sample, b) showing the spectral signature of the plastics material used for the 3D-printed ring, and c) a microscope picture showing a cluster of POM fibers

was 0.06 MPs/m^3 . For HSI, the mean concentration was $0.09 \pm 0.2 \text{ MPs/m}^3$ and the median was 0.0 MPs/m^3 . Variable concentrations displayed differences among the results from each instrument. However, there is no significant difference in the median of MPs concentration between the two instruments (K-W, $p > 0.05$, see Table B.1 in the Appendices). Hence, we can validate our assumption that

3. RESULTS

HSI measurements are equivalent to the FTIR measurements. Specific location differences were then investigated using the HSI results.

The mean concentration at *location A* was 0.1 ± 0.2 MPs/m³ and the median was 0.07 MPs/m³ with values ranging between 0.00 to 0.79 MPs/m³ whereas, at *location B*, it was 0.01 ± 0.02 MPs/m³ and the median was 0.0 MPs/m³ with values ranging between 0.000 to 0.06 MPs/m³. A higher MPs concentration tendency is observed at *location A* compared to *location B* (Figure 3.2.2). However, a significant difference in MPs concentration was observed between locations (K-W, $p < 0.05$, see Table B.1 in the Appendices and Figure 3.2.3).

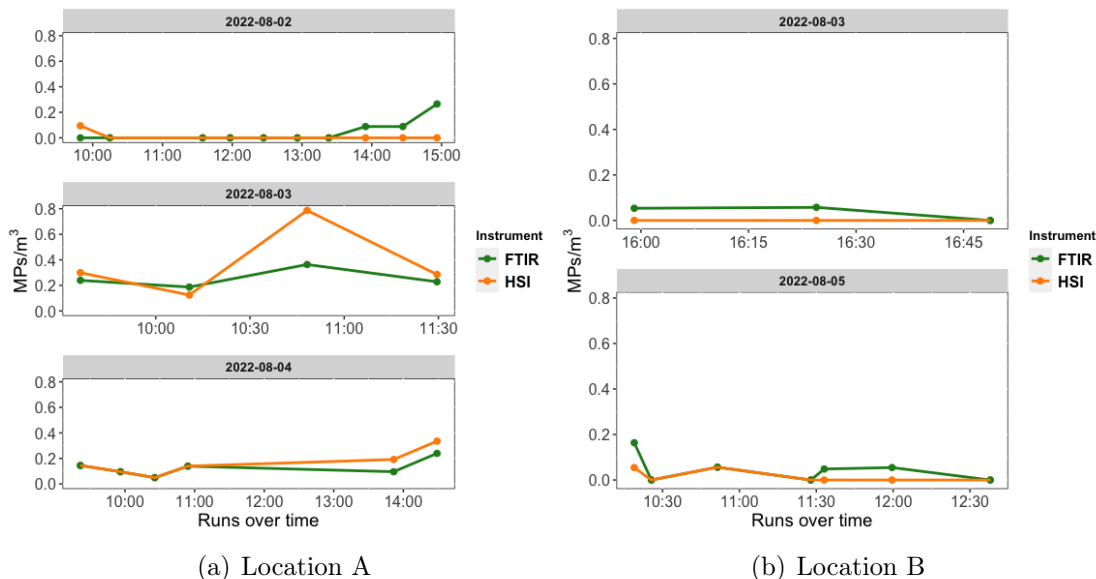


Figure 3.2.2: Distribution of MPs concentration (MPs/m³) over the field campaign period comparing both locations and instruments used.

Chemical and morphology characteristics of MPs found in Runde were investigated between instruments and locations. In all samples, seven different plastic polymers (PE, PP, PS, PMMA, alkyd varnish, phenoxy resin, polyester) were detected with FTIR and two (PE, PP) with HSI. PE was the most abundant polymer for both methods with 50% and 83% (3.2.4) and PP was the second most abundant with 37% and 17% for FTIR and HSI respectively. The diversity of polymers was higher with the FTIR results because HSI can only distinguish between four polymers (PE, PP, PET, PS). However, FTIR did detect one PS particle in Sample 34 whereas HSI did not detect any. By visual comparison, we investigated the differences between samples and found that for transects 22 and 30, HSI and FTIR detected the same PE or PP plastics particles [99].

Considering both instruments, PE and PP were the most abundant polymers found in Runde. The concentration of PPs and PEs per instrument was investigated and a significant difference was found for PP (K-W, $p < 0.05$) whereas no significance between instruments was found for PE (K-W, $p > 0.05$). Indeed, there are similar patterns observed in the samples compared to the spiked ones (see Section 3.1.2) suggesting a stronger detection of PPs by FTIR and of PEs by HSI [99]. Differences between locations were observed, but not significant (K-W, $p > 0.05$) with the HSI data where PPs particles are absent at *location B* (Figure 3.2.5).

3. RESULTS

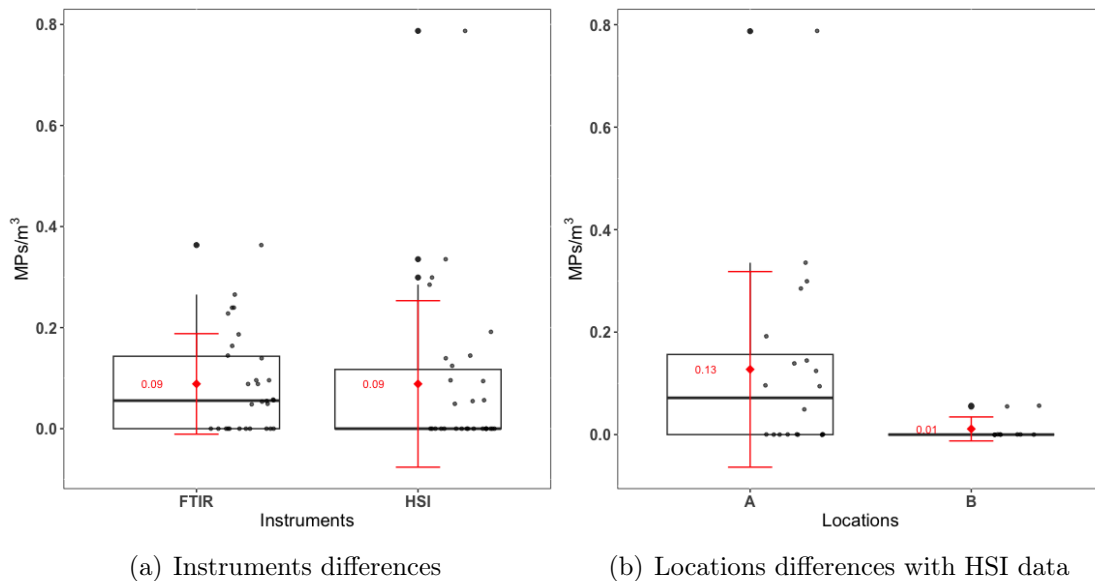


Figure 3.2.3: Comparison of MPs concentration per a) instrument (FTIR vs HSI) and per b) location (A vs B). Boxplot showing: interquartile range, minimum and maximum values, potential outlier, mean and SD of mean (red), and jitter of values per run are shown.

Shape classification can differ depending on the analysis method chosen. Visual inspection of particles under the microscope permitted shape classification for the FTIR results because of individual inspection of each particle and classification to a specific shape. For HSI, we followed Dawson et al [106] recommendations to calculate Feret max and Feret min ratio. If the ratio is bigger than 3, the shape of the particle is assigned to a fiber, if it is lower, the shape is considered to be a fragment. MPs particles are mainly fragments in both measurement methods (FTIR = 34 fragments, HSI = 45 fragments). HSI detected less fiber ($n = 3$) than FTIR ($n = 5$). Films ($n = 6$) and pellets ($n = 1$) were identified and characterized only by visual inspection under the microscope with the FTIR method (Figure 3.2.6). Overall, shape characteristics between instrument measurements are difficult to compare [56].

Plastics are distinctively classified by size. The early definition of MPs corresponds to plastics $> 300 \mu\text{m}$ and $< 5000 \mu\text{m}$ [54]. Hence, it is important to investigate the size distribution of MPs. For our study, the lower limit of MPs was set at $500 \mu\text{m}$ because of method limitation for quantification with the HSI [84]. For FTIR, the mean MPs size is $1308 \pm 786 \mu\text{m}$, and, for HSI, it is $1041 \pm 510 \mu\text{m}$. The MPs smaller than $1000 \mu\text{m}$ are most abundant for FTIR and HSI results (Figure 3.2.7). The findings from both instruments for MPs size ($> 500 \mu\text{m}$) are significantly different (K-W, $p < 0.01$). This is because FTIR detected a few meso- and macroplastics ($> 5000 \mu\text{m}$), (Figure 3.7(b), Figure C.1 in the Appendices). MPs quantification in size is mainly in the range of > 500 and $< 5000 \mu\text{m}$ (Figure 3.7(a)). There was no significant difference between instrument measurements in that specific size range (K-W, $p > 0.05$). Overall, nine MPs ($> 5000 \mu\text{m}$) are affecting the size distribution for the FTIR measurements. Excluding these particles, no significant differences were found between measurements and

3. RESULTS

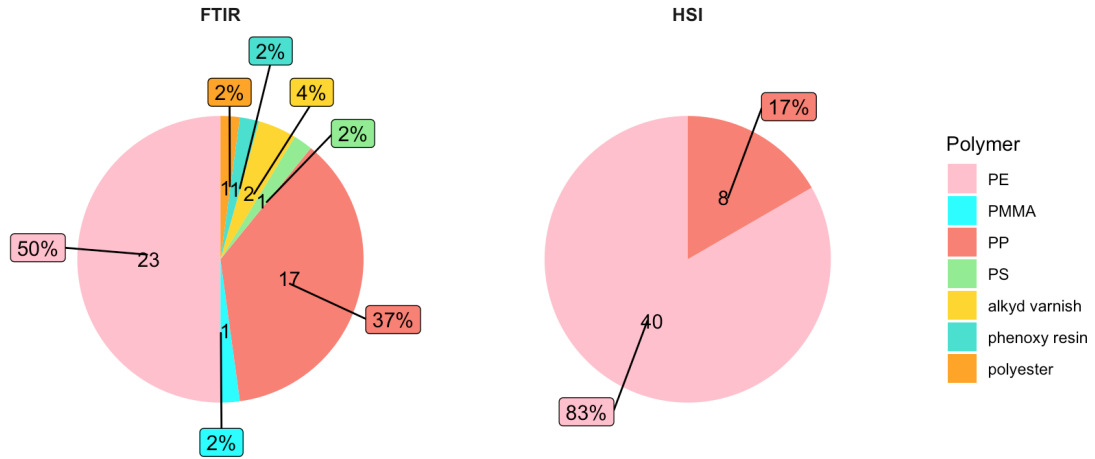


Figure 3.2.4: Comparing the polymer distribution of MPs for the two different analysis methods (FTIR vs HSI). PE: polyethylene, PMMA: polymethyl methacrylate, PP: polypropylene, PS: polystyrene.

locations (K-W, $p > 0.05$).

3.3 Diving in investigating the frequency of sampling and KEVs correlation

3.3.1 Frequency of sampling

Traditional MPs sampling protocols are known to be opportunistic, not taking into account ocean dynamics and what can cause variability in marine MPs concentration. Hence, our proof-of-concept study is trying to show the relevance and importance of sampling over multiple days with a high number of samples acquired per day.

On August 2nd, ten transects resulted in an average MPs concentration of 0.01 ± 0.03 MPs/m³ and a median of 0.0 MPs/m³.

On August 3rd, seven transects resulted in an average MPs concentration of 0.2 ± 0.3 MPs/m³ and a median of 0.12 MPs/m³.

On August 4th, six transects resulted in an average MPs concentration of 0.2 ± 0.1 MPs/m³ and a median of 0.14 MPs/m³.

On August 5th, seven transects resulted in an average MPs concentration of 0.01 ± 0.03 MPs/m³ and a median of 0.0 MPs/m³.

Standard deviation (SD) are all larger than the mean values except on August 4th (Figure 3.3.1). The SD from August 3rd is showing the highest variations probably due to the sampling at *location A* in the morning and *location B* in the afternoon. When investigating the medians, no MPs abundance was detected on August 2nd and 5th while MPs density was higher on August 3rd and 4th. A significant difference was observed between the days of sampling (K-W, $p < 0.01$). More specifically, when comparing days from different locations (August 4th vs 5th) or from different planned paths (August 2nd vs 4th), significant differences were confirmed (Dunn test, $p < 0.05$) with stronger variations explained by different

3. RESULTS

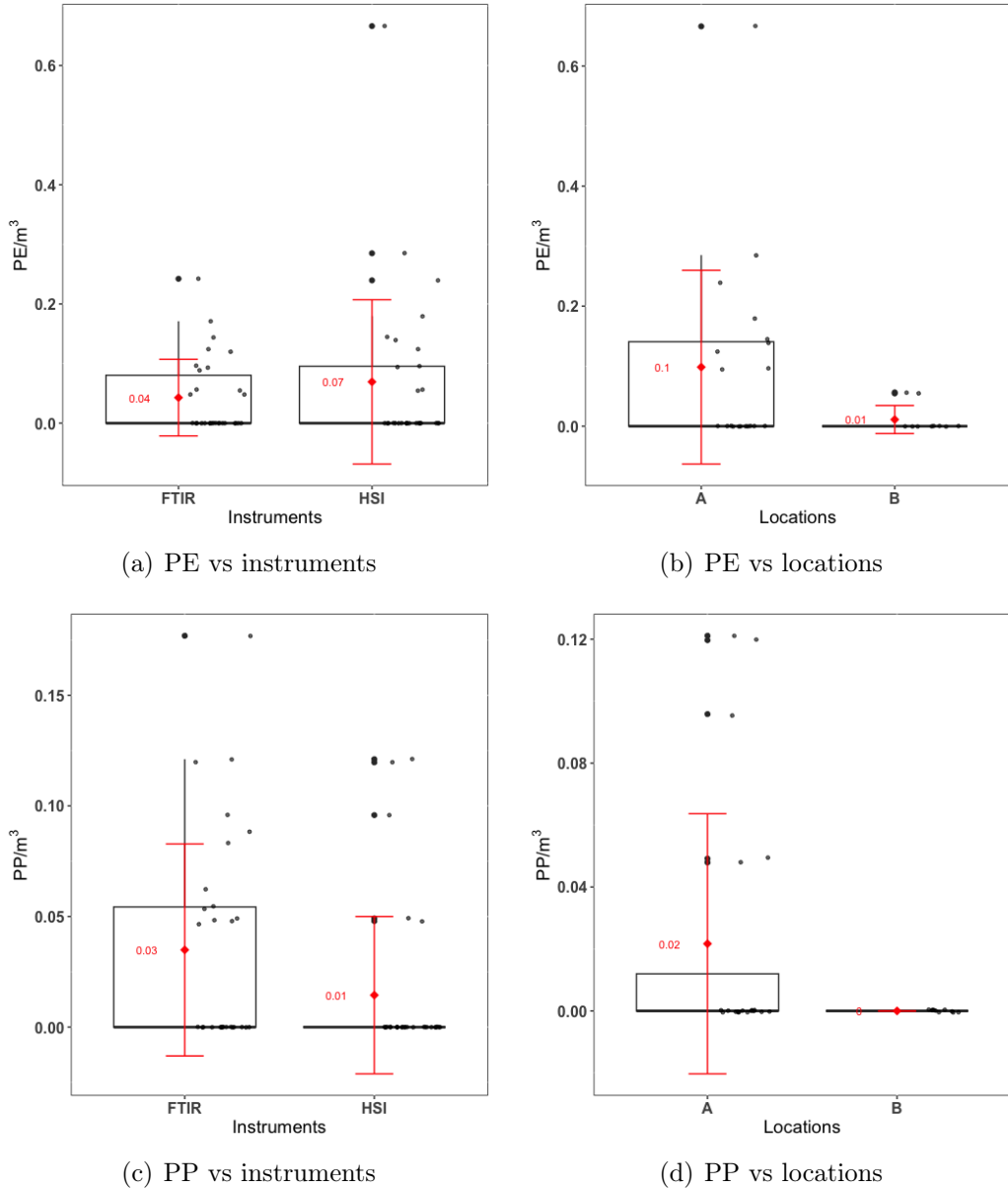


Figure 3.2.5: Comparison of polyethylene (PE) and polypropylene (PP) concentration per a) and c) instrument (FTIR vs HSI) and per b) and d) location (A vs B). Boxplot showing: interquartile range, minimum and maximum values, potential outlier, mean and SD of mean (red), and jitter of values per run are shown.

planned path.

3.3.2 Key environmental variables

We investigated the potential effect of tide level and wind speed on HSI MPs concentrations (Table 3.3.1). To see if any correlations occurred, linear regression model (lm) showed and scatter plots of the KEVS against MPs concentration showed that tide doesn't explain the variance in MPs concentration ($p > 0.05$)(Figure 3.2(a), and was therefore removed from the model. A significant and positive effect was observed for wind date ($p = 0.02^*$)($R^2 = 0.223$)(Figure 3.2(b)).

3. RESULTS

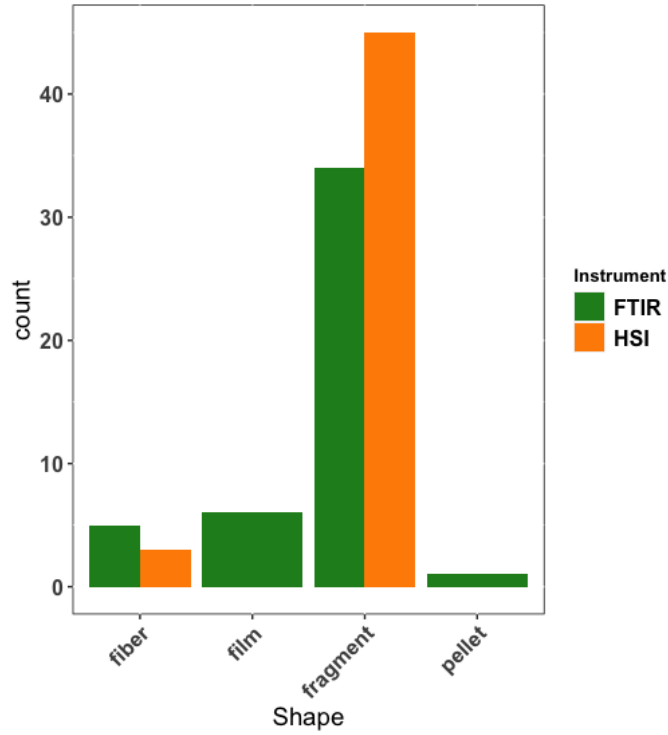
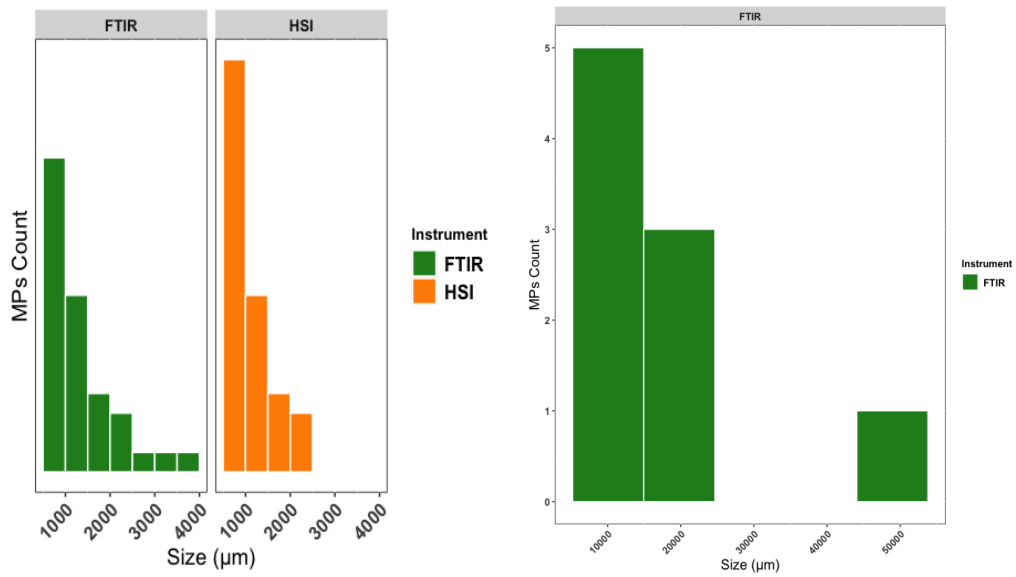


Figure 3.2.6: Microplastics variation in shape depending on the instrument used: FTIR (green) vs HSI (orange)



(a) Size distribution (500-5000 μm) of MPs (b) Size distribution (>5000 μm)

Figure 3.2.7: Size of microplastics (MPs) quantified by FTIR and HSI

Increased wind speed data may correlate with increased MPs concentration (Figure 3.3.3).

3. RESULTS

Table 3.3.1: Fieldwork summary with the corresponding KEVs data: Location A corresponds to the exposed location and B to the sheltered one. Wind data was taken from Svinøy Station (SN59800) and tide data from Runde fyr.

| Date | Location | Runs | MPs concentration (particles/m ³) | Win Speed (m/s) | Tide level (m) |
|------------|----------|------|---|-----------------|----------------|
| 02/08/2022 | A | 1 | 0.094 | 6.9 | 117.4 |
| 02/08/2022 | A | 2 | 0.000 | 6.9 | 129.6 |
| 02/08/2022 | A | 3 | 0.000 | 6.9 | 172.2 |
| 02/08/2022 | A | 4 | 0.000 | 6.9 | 180.9 |
| 02/08/2022 | A | 5 | 0.000 | 10.9 | 178.6 |
| 02/08/2022 | A | 6 | 0.000 | 10.9 | 185 |
| 02/08/2022 | A | 7 | 0.000 | 17.2 | 183.5 |
| 02/08/2022 | A | 8 | 0.000 | 17.2 | 179.8 |
| 02/08/2022 | A | 9 | 0.000 | 14 | 171.3 |
| 02/08/2022 | A | 10 | 0.000 | 14 | 157.5 |
| 03/08/2022 | A | 11 | 0.305 | 12.9 | 88.1 |
| 03/08/2022 | A | 12 | 0.299 | 12.9 | 106.2 |
| 03/08/2022 | A | 13 | 0.124 | 22.3 | 123.7 |
| 03/08/2022 | A | 14 | 0.787 | 22.3 | 147 |
| 03/08/2022 | A | 15 | 0.285 | 20.3 | 168.6 |
| 03/08/2022 | B | 16 | 0.428 | 19.4 | 184.6 |
| 03/08/2022 | B | 17 | 0.000 | 19.4 | 159.9 |
| 03/08/2022 | B | 18 | 0.000 | 16.4 | 149 |
| 03/08/2022 | B | 19 | 0.000 | 16.4 | 133.6 |
| 04/08/2022 | A | 20 | 0.145 | 12.1 | 69.1 |
| 04/08/2022 | A | 21 | 0.096 | 12.1 | 82.7 |
| 04/08/2022 | A | 22 | 0.049 | 9.3 | 92.15 |
| 04/08/2022 | A | 23 | 0.139 | 9.3 | 106.1 |
| 04/08/2022 | A | 24 | 0.000 | 14.2 | 128.3 |
| 04/08/2022 | A | 25 | 0.000 | 10.5 | 158 |
| 04/08/2022 | A | 26 | 0.192 | 11.5 | 173.6 |
| 04/08/2022 | A | 27 | 0.335 | 12.7 | 173.7 |
| 05/08/2022 | B | 28 | 0.055 | 15.4 | 75.3 |
| 05/08/2022 | B | 29 | 0.000 | 15.4 | 77 |
| 05/08/2022 | B | 30 | 0.056 | 15.4 | 86.9 |
| 05/08/2022 | B | 31 | 0.000 | 15.4 | 91.1 |
| 05/08/2022 | B | 32 | 0.000 | 17.3 | 105.9 |
| 05/08/2022 | B | 33 | 0.000 | 17.3 | 105.9 |
| 05/08/2022 | B | 34 | 0.000 | 17.3 | 120.8 |
| 05/08/2022 | B | 35 | 0.000 | 17.4 | 139.5 |

3. RESULTS

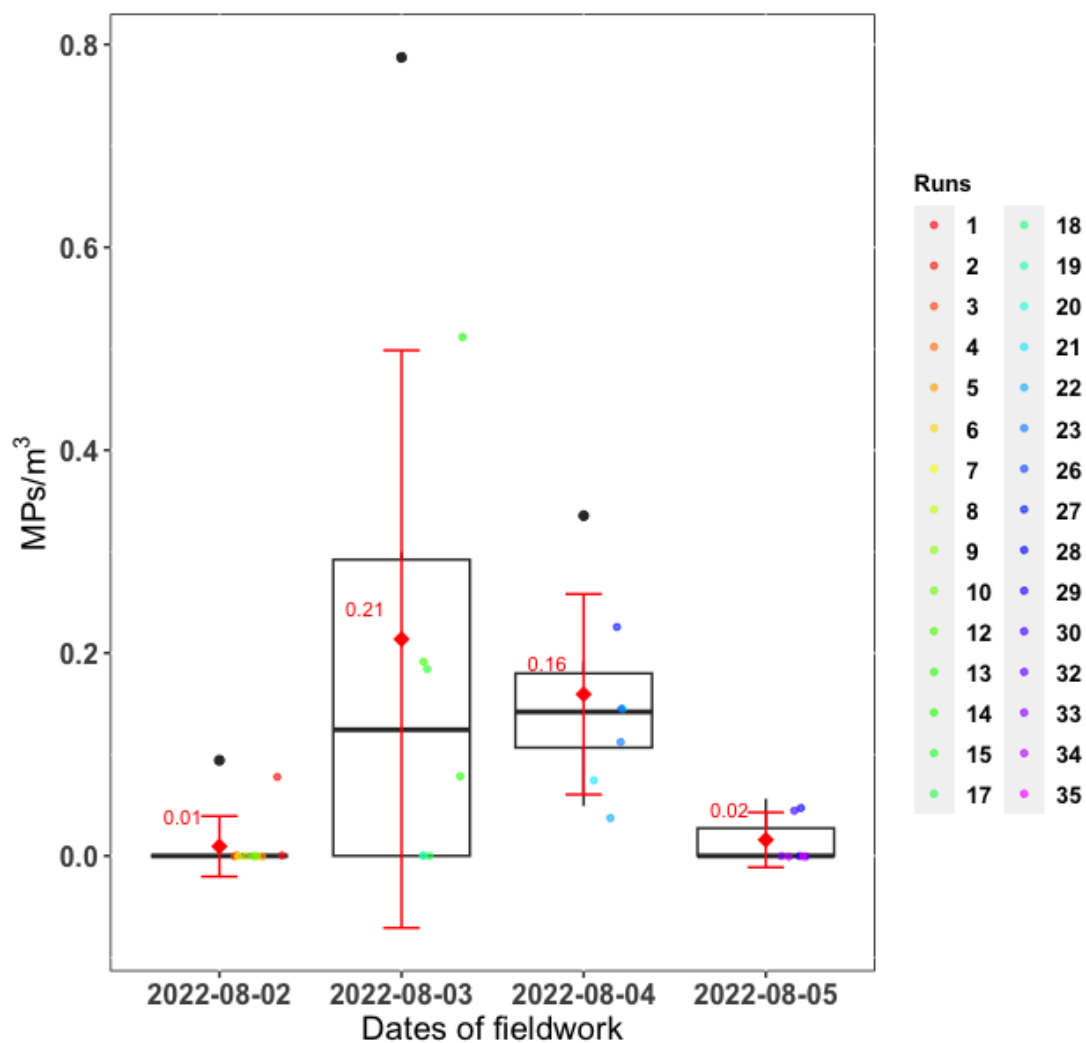


Figure 3.3.1: Comparison of microplastic concentration (MPs/m³ per dates of fieldwork). Boxplot showing: interquartile range, minimum and maximum values, potential outlier, mean and SD of the mean (red), scatter dots coloured respectively by runs.

3. RESULTS

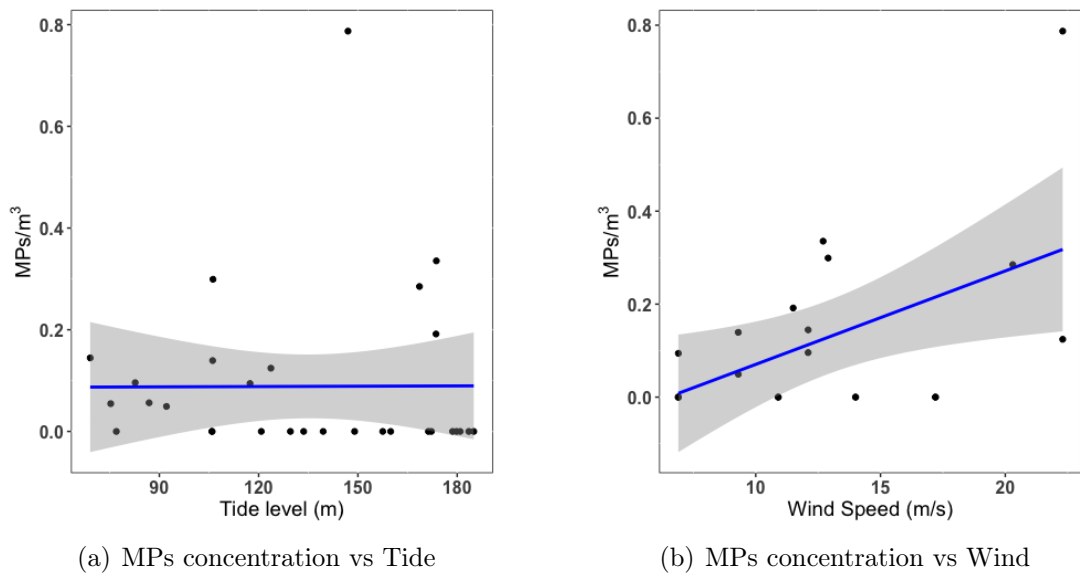


Figure 3.3.2: Investigation of microplastics (MPs) concentrations potential correlation to the key environmental variables (tide and wind speed). The trendline follows an lm model with standard error.

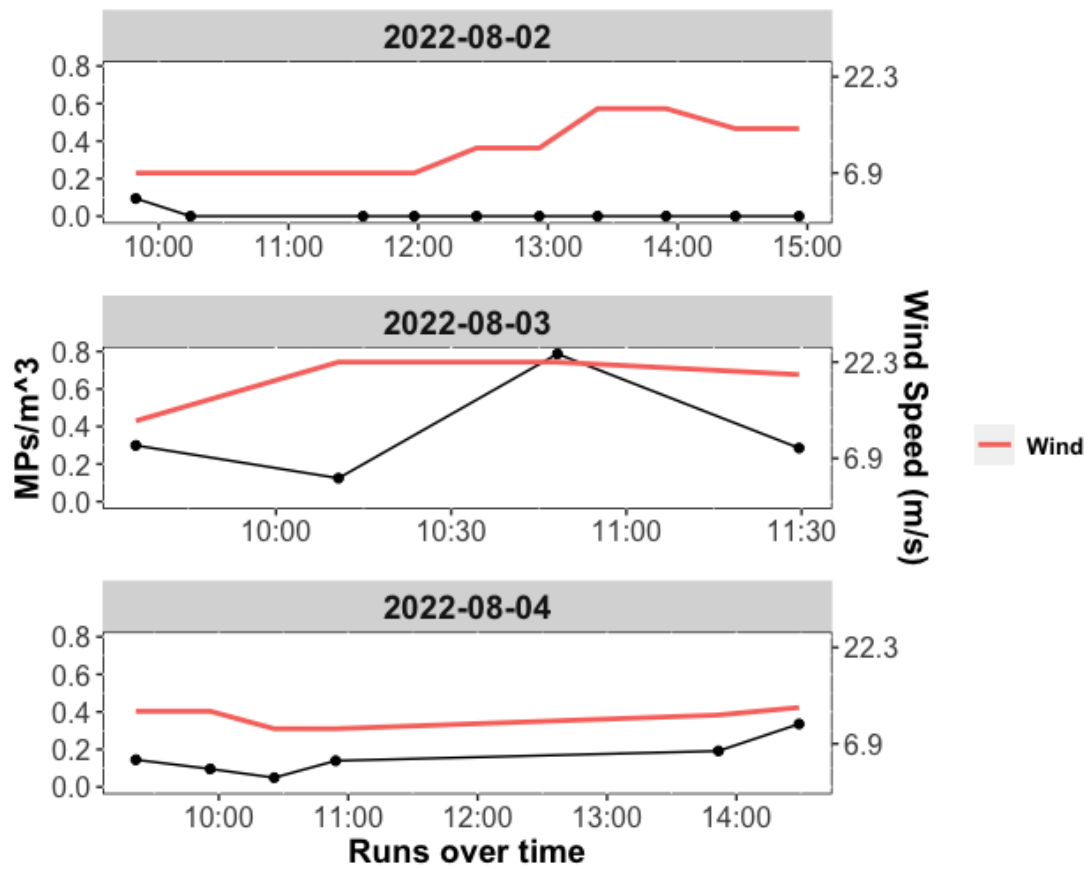


Figure 3.3.3: MPs concentration (MPs/m³) compared to wind speed at Location A over the field campaign period.

4.1 Methods Performance

The combination of PCD and HSI methods for measuring surface water MPs concentration is aiming to address previous method limitations regarding sampling and analysis of MPs through a more reproducible and repeatable methodology (RAPs).

4.1.1 Net advantage of using a robot and a hyperspectral imager compared to common methods used in MPs research

The PCD is an advantageous method compared to a common manta net normally used for MPs sampling [80]. Throughout the field campaign, no boat was used, which is traditionally required to tow the manta net, reducing the amount of time and logistics, and avoiding the need for a vessel crew and cost related to it.

Moreover, remote, narrow, and shallow areas are harder to access with a boat which was not the case with PCD since it was perfectly capable of being carried by one person over rocks and cliffs to reach small bays (see Figure 2.2.1) or launched from a pier at low tide when water levels were more shallow over longer spatial distances at *location B* (for reference, see Figure 4 in Zolich et al. 2022 [88]).

Additionally, turbulence by the boat's speed and weather can alter the performance of a simple manta net. However, our robots are propelled by two thrusters located underneath and behind the mouth minimizing turbulence caused by an external factor instead of only KEVs [88]. Moreover, the PCD did not encounter any struggles with strong winds and high waves specifically whereas using a typical manta net from a boat, the condition needs to be fairly calm as the boat is already causing turbulence in the water [80].

Unique advantages can also be gained while using a PCD for MPs sampling. To operate the PCD, no prior knowledge of computer science and engineering is required, only a few hours of training is sufficient allowing researchers from different fields to use the robot for their research. It can be operated by two people on-site only where one can launch the vehicle in the water while the other

4. DISCUSSION

person drives it out and sends it in autopilot mode. Even kids during fieldwork were able to successfully drive the robot to shore. A robotics expert can connect remotely through the mobile network and be able to intervene when errors occur while the robot is in autopilot mode (see Figure 3.1.1).

Another advantage is to be able to plan a specific path which helps design the perfect sampling route to answer a specific research question and its objectives. For this proof-of-concept study, 300 m, 600 m, and 680 m identical circular transects were planned. On the first day of sampling, at *location A*, a shorter transect (300 m) to test the performance of PCD. Although the weather was harsh, the robot did not encounter any struggles with strong winds and high waves and clogging of the net was minimised on the first day, hence, we decided to double the distance for the other days at that location. Indeed, clogging of the net is a big issue in MPs sampling [107, 80]. The challenge is to find a balance between sampling enough water for a representative concentration of MPs without encountering too much clogging of organic matter in the net which can affect water intake due to more resistance in the net and, as a result, falsifying volume measurement. The net attached to the PCD is a common manta net that one would use for MPs research from a boat [88]. The cod end, however, was specifically designed larger to allow for high organic matter and marine litter to be collected in it, so large even a jellyfish got caught in it twice (runs #13 and #20) without affecting the quality of the sample!

The interchangeable equipment available for field work includes eight batteries and six cod ends allowing for consecutive sampling throughout a day without access to electrical power. On top of that, three identical PCD were available allowing for replacement of the robot quickly if any troubles or overheating in the electronic box occurred. In addition, runs 28-33 were tested using two units at the same time. Two units were launched approximately five minutes apart resulting in more accurate replicates as it is often a forgotten or overseen parameter in MPs sampling [80]. Running this kind of experiment simultaneously at the two different locations on Runde Island would have helped to provide a better holistic understanding of MPs concentration, especially during extreme weather events.

Other researchers have tried to address the known limitations of surface water MPs sampling [108, 87]. Like us, they are mainly trying to target the lack of a standardized method for MPs sampling across all water bodies. Both studies compared thoroughly the performance of their new prototype to the traditional manta net concluding that the use of a boat and the limitation of the mesh size of the net are major limitations to MPs findings. Comparing the PCD to these devices can help assess its strength compared to the traditional method and other innovative methods (see Table 4.1.1). Keeping the idea of implementing a high-throughput sampling procedure, the autonomous feature, the net lifting addition, the customised cod end, and the three identical units with sample containers and interchangeable batteries make PCD a good candidate for future surface water MPs research. Even the aquatic drone was tested in another water body than coastal waters [109], proving that PCD would potentially be an asset for future river studies that usually need a bridge to deploy the net [110].

Overall, the PCD units have both advantages from the grab sample, from the manta nets, and new devices (see Tables 4.1.1 and 1.3.1) as they can cover larger

4. DISCUSSION

Table 4.1.1: Comparison of two other prototypes for MPs sampling to the one used in this study. All devices are trying to address current limitations related to the Manta Net.

| | MuMi [108] | Jellyfishbot [87, 109] | PCD [88] |
|---|--|---|--|
| Operation | Need a boat, restricted areas, affected by boat disturbances | No boat required, any water bodies with shallower depth at lower cost | No boat required, can access restricted and protected areas at lower cost |
| Extra features | Interchangeable filters (50-500 μm) for easy replicate sampling | Stable catamaran structure, using a remote control for sampling, interchangeable net (150-300 μm) | Stable catamaran structure capable of withstanding tall wave heights (> 1 m), lowering/lifting of the net possible, interchangeable net (100 - 300 μm) |
| Volume measurement accuracy | Built-in flowmeter and able to see the volume while sampling from the vessel | Common flowmeter attached to the frame and one attached to the propulsor | Common flowmeter attached to the frame and GPS data for comparison |
| Average volume filtered per sample | 0.370 m^3 | 32 m^3 | 14.4 m^3 |
| Frequency of sampling | 6 transects at 1 location | 3 replicates for each of the 2 locations and at 3 different months | 4 days with 8-10 samples per day at 2 locations |

spatial ground in less time, analyse more volume, and have a high-frequency sampling throughout the day [79, 70, 80]. Indeed, it was shown that sampling a smaller water volume using the MuMi device overestimated the concentration found compared to the Manta net [108], hence, the need to keep a higher volume using an automated or autonomous device like the JellyfishBot [87, 109] and the PCD used in this study [88].

More replicates throughout the day can also help keep a high enough number of replicates to reach an acceptable precision of MPs concentration [99, 111] in the situation where transects were incomplete due to some errors (see Figure 3.1.1). For this fieldwork, except the first day (2022-08-02) with the smallest planned path, we encountered difficulties resulting in losing one or two samples per day and/or location. Nonetheless, the lowest amount of samples that we had per day was six (see Figure 3.3.1 and Section 3.3.1). Six samples per day are higher than

4. DISCUSSION

most of the current research on surface marine MPs using a manta net if the number of replicates is even mentioned in the study [107, 108, 80].

To assess the performance of the HSI, the overall experience and the type of results obtained were compared to a common method used [76]: visual inspection under microscopy and FTIR spectroscopy.

An impressive time efficiency with the HSI method resulted in five times faster (25 h) MPs analysis of all samples collected during the fieldwork. This is a major progress compared to the FTIR method where 67% of particles handpicked are unconfirmed leading to a much longer analysis time (130 h). This non-invasive and non-destructive method is pushing the limits of ecology and MPs research surrounding the 3Rs: repeatability, replicability, and reproducibility [112, 76]. Using HSI improves all three since the SIMCA model can be used by anyone provided with the code reducing any operator errors we have during visual inspection of MPs under the microscope with the FTIR method. Indeed, visual characterization as part of the FTIR method is very objective. Bias can be introduced if the researcher has no experience compared to an expert in the field [113, 114].

Validation of HSI with the spiked samples was successful as no significant difference between the FTIR and the HSI methods was found [99]. Both methods, however, underestimated the MPs abundance compared to the true value potentially due to laborious and tedious laboratory steps and time-demanding analysis leading to a potential underestimation of MPs [115].

False negatives and false positives were also encountered for both methods. Different factors can explain the difference in the recovery process like the loss of particles, differences in the spectroscopy techniques, and different spectral databases used to match the particle spectra to a specific polymer type. Both methods detected the same amount of PET, but only corresponding to 33% of the true value in the spiked samples. One lost particle was recorded with the FTIR method before it could be characterised. This particle might be the missing PS particle that HSI did detect and FTIR did not. HSI missed PP classification and detected more PE than FTIR probably due to the similarity in their chemical fingerprints and functional groups suggesting that some PP might have been classified as PE (see Figure 3.1.3, Figure 3.1.4, Table 1.2.2) [84, 92]. Other than the extra patches detected with the PET plastics under the HSI and the overestimation of PE, no other false positives were detected proving that the choice of a SIMCA one-classification model is efficient in avoiding an overestimation of MPs particles [92].

Overall, it is impossible to quantify the missing MPs in this study as the MPs laboratory processing steps are not the main focus, but it should be considered in the future for a better RAPs approach [115].

4.1.2 Addressing limitations: towards implementing reproducible analytical pipelines

RAPs and TRLs are needed for validating and harmonizing MPs monitoring globally [85, 99]. Hence, we address the limitations encountered during this research with the PCD and HSI validated with FTIR so we can propose solutions for further optimisation.

4. DISCUSSION

An important aspect of marine MPs research is calculating the volume of water filtered through the net. Traditionally, this is done with a flowmeter attached to the metal frame of a manta net [70, 74, 80]. We recorded the volume with a flowmeter as well, attached in the middle of the mouth frame for the net. However, studies have questioned the exactitude of these measurements because tracking the volume sampled is challenging because the water height can change a lot during a transect since it can be influenced by wind, wave height, and even resistance from the dragging or clogging of the net [108, 80]. The PCDs are initially designed to have the metal mouth opening of the net in a horizontal position fully submerged when in undisturbed waters [99, 88]. This could be further investigated using a mounted camera on the frame of the PCD to validate the water height in the net and adequately calculate the amount of volume filtered per samples [116] and recording it for more accurate calculation of filtered volume [117].

Contamination of MPs from sampling and processing is still a big issue [106]. The ubiquity of MPs is the principal issue as it is found everywhere from the atmosphere down to the deepest part of the ocean [68, 69, 1, 32, 14]. Typically, a researcher would implement a thorough QA/QC protocol to avoid any type of contamination that can come from a boat or the laboratory extraction. For the PCD, the net opening was purposely placed in front of any plastic material in the robot. The lifebuoys used as the floating catamaran structure are orange for easy detection of contamination [99, 88]. One contamination was detected and came from the robot itself. A 3D-printed POM ring was made for easy attachment and removal of the cod end to the net. However, screwing and unscrewing the cod end with this plastic ring resulted in the accumulation of shredded fragments, clusters of fibers, and fibers particles in the cod end and, therefore, in the samples and the blanks (see Figure 3.1(a)). Hence, the exclusion of the POM particles found was decided because it is also a plastic that is dense in seawater and, hence, unlikely to be part of surface water concentration (see Table 1.2.1). This detection was only possible with the FTIR analysis method as it can detect more polymers than the HSI method which can only detect four (PE, PP, PS, PET). Moreover, the colours of MPs are only recorded when visual inspection and identification are done under the microscope with the FTIR method.

Lastly, the implementation of PVC in the spectral database of the SIMCA model succeeded although a wider variety of samples is needed to reduce the number of cluster particles that can be seen in the PCA (see Figure 3.1.4) [84] and, therefore, increase the accuracy of the model. Moreover, other studies have shown successful classification of polymer type when more than four polymers are included in the model [91, 92].

In conclusion, the PCD is a strong competitor to the traditional Manta Net and other new devices being developed. When the certainty of volume measurement is investigated and the specific source of contamination due to the POM plastic ring attached to the cod end is resolved, the autonomous vehicle will be a great asset for researchers trying to increase their sampling frequency with a limited budget and crew and without compromising the accuracy and compatibility of the data collected. Additionally, as of now regarding the use of HSI and multivariate models for spectral classification of MPs, the HSI method still has systematic

4. DISCUSSION

weaknesses compared to the FTIR method. Hence, if, in the future, advances in the research come across those limitations, HSI would be the viable, more reproducible, repeatable, and comparable method for a rapid analysis of MPs samples. Hence, together, the PCD and HSI are an innovative combo towards RAPs in MPs research.

4.2 Hyperspectral imager for environmental monitoring of microplastics

4.2.1 Analysis comparison and spatial differences: both instruments gave the same results, and the microplastic concentrations may vary at different locations

MPs concentrations per transects throughout the field campaign were highly variable (see Figure 3.2.2). The variability in MPs concentration was captured by both instruments as no significant difference was found. This is a positive result for the validity of the HSI over the common FTIR method for the detection and quantification of MPs in the environment. As seen in (see Figure 3.2.3), more than 50% of the values correspond to a non-presence of MPs which resulted in a null median. Nevertheless, additional analysis verified the existence of MPs particles in certain samples, highlighting the considerable variability in MPs concentration at Runde. This variability suggests that, at times, no MPs are collected, while at other times, concentrations are significantly higher. This underscores the importance of a higher sampling frequency to capture and understand the dynamic nature of MPs in the environment.

Further investigations between instruments were made looking at the difference in polymer classification. PMMA, alkyd varnish, phenoxy resin, and polyester were found in small amounts (see Figure 3.2.4). As seen in Table 1.2.1, these plastics have different applications and can be related to the location where they were found. At *location A*, phenoxy resin and PMMA were found indicating a potential link to antifouling paints and coatings from the shipping industry underlying a potential long-range source of MPs from the open ocean to coastal ocean [118, 119]. At *location B*, the side of the island less affected by the weather but more affected by urban runoff, the presence of alkyd varnish was observed, potentially linked to wood coatings from a pier, or a boat house. The identification of polyester aligns with its common association with textiles, making its presence logical in a location affected by human activities [8]. If the LOD was lower, a higher amount of polyester could potentially have been found as it is proven that a significant proportion of plastic pollution is microfibers (where polyester is predominant) from textiles [82, 120]. As polyesters' shape description are fibers, the HSI instrument used here have shown limitations in detecting long and thin MPs shapes (see Figure 3.2.6). With the HSI limitations related to the detection of fibers [76] and the LOD of the mesh size of the net (300 μm), our concentrations are probably underestimating the abundance of MPs in the Norwegian sea [121]. Distinguishing between only fibers and fragments with HSI is ambiguous and doesn't take into account the variable shape characteristics that MPs can have in the marine

4. DISCUSSION

environment due to weathering and ocean dynamics [122, 123]. An optimisation is needed for the classification of shapes with the HSI MPs as proposed by Liu et al (2023) [56]. Even further 3D characterization could be useful for correlation with ecotoxicological studies, hydrological data, and transport dynamics as it can be influenced by MPs physical characteristics, such as shape [66, 56, 63].

The other three polymers found were PE, PP, and PS. Those results are comparable between the instruments since HSI can detect them. However, the PS particle found by FTIR was not classified by HSI. From the recovery test using the artificial seawater spiked MPs samples (see Figure 3.1.3), we have found that HSI detects more PEs than FTIR and FTIR detects more PPs than HSI although not statistically different [99]. These findings were also made in the environmental samples. Since the environmental data has no true value associated with it, it is impossible to assess the accuracy of these findings. The median concentration of only PP and PE were investigated further noticing that there was a significant difference between instruments for PP concentration. This might be related to the fact that PP particles found in the samples were thin films (see Figure C.1). Thinner films can be a cause for false negatives because their signal is not strong enough for the HSI to detect it properly.

Moreover, PE and PP particles are the most abundant polymers often in surface marine environments due to their relatively low density, and their popularity as a material for packaging [124, 125]. A few studies have started to classify the abundance of PE:PP copolymers in the marine environment [126, 127]. Hence, polymer blends could also be other limitations to the HSI model, and, potentially for open source libraries, like OpenSpecy [105], since Primpke et al. (2020) also noticed differences in PE and PP particles between different instruments used [128].

Another potential cause of the variations in the detection PE particles between HSI and FTIR is the wide range of polymer characteristics associated with PE. Indeed, using the spectra from the FTIR results, for some particles, we were able to distinguish between HDPE and LDPE with an open-source library like OpenSpecy [105]. This is done by investigating the presence or absence of the peak at 1377 cm^{-1} and the relative heights of the peaks at 1471 cm^{-1} and 1464 cm^{-1} . In our samples, out of 49% PE particles, 11% were confirmed as LDPE and 9% as HDPE. On the other hand, HSI is regrouping in the SIMCA model LDPE and HDPE in one category: PE. Distinguishing between these types of PEs is important for helping to monitor the success of waste management techniques [124, 129] as LDPE was found in higher percentage due to its lower recycling rate. It was recently proven that the branching difference in LDPE and HDPE polymers' structure can help to distinguish their spectra from HSI due to small overtone variations linked to the difference in linearity, density, and crystallinity [130]

In conclusion, MPs concentrations varied significantly per transect during the field campaign, with both HSI and FTIR methods effectively capturing this variability. No significant difference was found between the two methods, supporting the validity of HSI for MPs detection. However, our analysis at Runde revealed sporadic MPs presence, emphasizing the need for a higher sampling frequency. Polymer classification differences highlighted associations with specific sources at different locations. Methods and mesh size limitations may result in underestimating MPs

4. DISCUSSION

abundance in the Norwegian Sea. Notably, distinctions between PE particles and the prevalence of thin PP films present challenges for accurate detection. Addressing these limitations is crucial for effective MPs monitoring and waste management assessments.

4.2.2 Transport dynamics may influence spatial differences at Runde: exposed location contains a higher density of microplastics

Transport mechanisms in the coastal seas surrounding Runde are influenced by various factors, including the island's bathymetry, tidal transport, wind-driven drift, Ekman circulation, and wave/wind direction. Additionally, surface MPs are known for their ability to undergo long-range transport and settle on coastlines and ocean gyres [18, 131]. These factors collectively account for the observed variability in MPs concentrations in samples collected from the same location and following the same path at different times (see Figure 3.2.2)[63]. Notably, the MPs concentration was significantly higher at the exposed *location A* than at the sheltered *location B* resulting in a wider range of concentrations from the minimum value of (0.000) to the maximum of (0.787) (see Figure3.2.3).

The highest variability of MPs concentration was at *location A* suggesting that the NAC transports MPs from more heavily polluted regions to the Norwegian coast, where it interacts with the NCC [132, 98, 133, 134]. *Location A* is characterized by its exposure to prevailing south-westerly winds [135] and disturbances from waves and currents [97, 96]. Surface MPs are known to have long-range transport and settle on coastlines and ocean gyres creating several hot spots in the ocean and on islands on the coast [18, 131]. Furthermore, factors contributing to this variability may include the gentle slope and the sheltered bay where *location B* was sampled, which restrict mixing and Stokes drift effect resulting in lower variability of MPs concentration.

Overall, waters surrounding Runde exhibit variable MPs concentrations that could be influenced by complex transport mechanisms. KEVs. such as prevailing winds, water level, and currents may contribute to higher concentrations at exposed locations, while sheltered areas show lower variability due to restricted mixing. This is why we further investigated the correlation between tide and wind speed with the abundance of MPs.

4.2.3 Relevance of microplastics concentration detected at Runde compared to other studies

While comparing our findings to other studies is important, discrepancies between methods, locations, and reported units can complicate the comparison. Hence, the studies chosen here either followed a similar sampling method to ours to notice similar trends or explained a different variation in MPs concentration related to a different location and/or sampling method.

In the Northern and Norwegian Seas, some research investigated the concentration of marine MPs along the Scottish, Danish, and Norwegian coastline [72, 67]. In

4. DISCUSSION

the NOAA global marine plastics database, MPs concentrations observed range along the Norwegian coast are spanning from a very low ($0-0.0005$ MPs/m³) to a medium ($0.005-1$ MPs/m³) concentration [67]. Our study reveals that our mean MPs concentration (0.09 MPs/m³) falls within these observations.

While most of the samples in the NOAA database [67] were collected opportunistically, one notable instance of MPs concentration was at Runde, the same location as this study, where Faure et al. (2015) [136] during a sailing cruise, reported a concentration of 0.366 MPs/m³. Additionally, Russel et al. (2021) [137] did a high temporal and spatial study in Scotland waters where 398 stations were investigated over six years (2014-2020). They found a concentration ranging from 0 to 1.215 MPs/m³. Areas where hotspots were discovered are most likely exposed to the coastal current transporting MPs on the west side of Scotland showing a similar tendency as for our exposed western location (A) at Runde. This study also reported mostly fragments as it has a similar LOD as our study due to the mesh size of the nets used.

Furthermore, another study, by Gunaalan et al. (2023) [138], conducted in Danish waters, specifically the Kattegat/Skagerak region, demonstrated notably higher concentrations ranging from $11-87$ MPs/m³. This variation underscores the substantial differences in transport mechanisms between open coastlines and semi-enclosed seas. In areas with more limited water circulation, such as the Kattegat/Skagerak, MPs tend to accumulate [139], resulting in elevated MPs concentrations. It is worth noting that most studies [138, 80, 137] mentioned calmer weather conditions during their sampling campaign in contrast to the strong winds and rain experienced during our field campaign. This discrepancy suggests that extreme weather events during fieldwork may have an impact on MPs concentrations and distribution. Moreover, they also used an in-situ pump that could explain differences in the MPs abundance obtained since this sampling instrument often collects more subsurface waters which shows a different distribution of MPs than at the surface [140, 141].

Globally, surface MPs concentration tends to be higher near continents compared to open ocean [32, 134]. When comparing our MPs abundance on a global scale, relative MPs concentrations along the Norwegian coast are relatively low compared to more populated coastal areas, such as the Mediterranean [32, 67]. Keeping in mind our LOD of 300 μm , we might be underestimating the abundance of MPs at Runde. Pakhomova et al. (2022) [141] studied subsurface waters from the Arctic to Antarctica. They indicate with their results that the Northern Hemisphere is more polluted by fiber since it can be transported by air and water compared to fragments that are usually limited to the water mass they come from. This is another reason why recording shape and size is important, and why it should be better implemented with the HSI method since it can help explain transport dynamics.

Studies have been uneven and scarce in general on the Norwegian coast which makes the evidence of plastic pollution less visible compared to other well-known hotspots [32]. However, islands have been shown to accumulate plastic debris on their shorelines which, in turn, would indicate the presence of MPs [142]. Moreover, Cózar et al. (2017) [143] suggested that the poleward branch of the thermohaline circulation is participating in the long-range transport of plastic debris

4. DISCUSSION

from the North Atlantic to the Greenland and Barents seas (see Figure 1.3.1). This finding can also be seen in Pakhomova et al. (2022) [141] (for further reference, see figure 6 in this paper) where the weight concentrations were both higher for Central Atlantic and Barents sea water masses compared to the North Atlantic, Antarctic, and Siberian ones. We can hypothesise that although northern latitudes have been overlooked for MPs pollution due to the lack of important nearby pollution sources, plastics can be transported from heavily dense populated areas to remote areas.

4.3 The relationship between key environmental variables, frequency of sampling, and microplastic concentrations

High variation per day of MPs concentration (see Figure 3.3.1) indicates that different drivers are responsible for the highly dynamic distribution of MPs. Indeed, geological, hydrological, biological, and meteorological factors can influence the high variability and heterogeneity of coastal marine environmental concentrations and distribution of MPs. We want to show why doing multiple days of fieldwork with a high frequency of sampling per day is important for a good and representative amount of replicates, especially for regions with a relatively lower MPs abundance and high variability [99].

KEVs investigated alongside the concentration of MPs were tide level and wind speed. While tide level was investigated over both locations (A and B), no correlation was found indicating that other factors could have more effect on the abundance of MPs in the region (see Figure 3.2(a)). On the other hand, a positive correlation was found between the abundance of MPs at *location A* and the wind speed recorded at that station 18 km away from Runde. This is following our findings since the highest variability of MPs concentration was at *location A* and, for both instruments, the highest concentration was found at *location A* on August 3rd corresponding to transect #14 (0.363 MPs/m³ for FTIR and 0.787 MPs/m³). It also corresponds to the highest recorded wind speed value during the fieldwork (see Figure 3.3.3). Frias et al (2020) [58] also showed that wind speed and direction can interact with the presence of MPs which can affect their transport from one environment to the other. Hence, when investigating on a smaller scale, the distribution and concentrations of microplastics (MPs) can be explained also by various local factors, including weather events, tidal regimes, riverine inputs, and seasonality. During the summer, the stratified waters experience mixing due to changes in local weather events, where the upper layer is more exposed to winds, tides, and temperature, facilitating the flourishing of biological processes. Indeed, even if our concentration was not correlated to the tide, other studies have found a correlation to tidal dynamics and MPs coastal transport when longer temporal scales are investigated (over months, seasons, and years) [123].

As depicted in Figure 3.3.1, the high daily variation in MPs concentration suggests that different physical drivers contribute to the highly dynamic distribution of MPs. A subtle trend was observed when comparing the windward side, *location*

4. DISCUSSION

A, to the leeward side, *location B*, with *location A* showing a higher abundance of MPs and more variable MPs concentrations, likely due to its exposure to wind, waves, and current disturbances. Extreme weather events can severely impact the concentration of MPs in surface waters by several mechanical processes, especially over longer temporal scales, such as seasonal variations [122]. Investigating the spatial and temporal dynamics of MPs can also help to provide essential information for risk assessment regarding toxicity with MPs ingestion [51].

An emerging concern for marine ecosystems like Runde is the potential impact of EDCs associated with chemicals in MPs [52]. EDCs, which include additives found in plastics, can leach into the marine environment and quickly accumulate in organisms leading to reproductive deficits [144, 145]. As Runde is known to be a nesting and protected island for seabirds, Biamis et al. (2021) [52] reviewed several studies reporting different seabird species where EDCs were found in various tissues, primarily assessing the physical ingestion effects. Tests conducted with MPs from the Norwegian coast have shown sublethal size effects in Japanese quail populations [146]. The concentrations of MPs reported in our study are lower than those examined in toxicological laboratory studies on the adverse effects of EDCs. Indeed, there is a need for more ecologically relevant research where environmentally relevant concentration should be tested in ecotoxicological studies [147]. As MPs concentrations are likely to increase, additional stressors on already endangered species in Runde could influence population dynamics. Additionally, MPs aspects, such as the predominance of the smaller size range in the environment (see Figure 3.2.6), can also be alarming regarding bioaccumulation of MPs in the food web [148]. At Runde, primary productivity and algal blooms were reported [149]. Those micro-organisms have a similar size range to MPs [8], hence, can interact, agglomerate, and/or ingest MPs while being at the bottom of the food web and a prey of different marine organisms.

Overall, investigating environmental concentrations at a larger spatial and temporal scale on biodiversity-rich islands like Runde can contribute to the preservation of marine ecosystems. Therefore, there is a clear need for further research to link adverse effects and environmental MPs concentrations in seabird-nesting islands.

In conclusion, further investigations and models are needed to investigate any other additive effects or interactions of other KEVs with the wind data could have on MPs concentrations at Runde. Sutton et al. (2016) showed that increased rainfall and stormwater runoff can in turn increase MPs concentration. Precipitation and terrestrial runoff could be investigated in addition to wind data, for instance, a generalized additive model (GAM) could have been used to understand how KEVs interact together to explain the distribution and variance of MPs concentrations [150]. As climate change is exacerbating extreme weather events globally, it should be a priority to understand MPs distribution when those weather events occur to prevent any extra input of MPs pollution in the ocean.

4.4 Outlook and future work

This proof-of-concept study was trying to address limitations in the MPs research world. Overall, the combination of PCD and HSI is a step towards a more reproducible, repeatable, and comparable method for surface marine research. We assess that, by the successful application of our technologies, the PCD was evaluated at a TRL of 6 and the HSI at level 4-5 as it is still in the applied research phase and not completely to the level of the other analysis tool [85, 99]. A concrete RAPs is needed to apply the PCD and the HSI in future research.

We proposed a thorough protocol ensuring all limitations encountered must be avoided in the future and suggesting further optimization of the technologies.

1. MPs sampling: Higher spatial and temporal sampling frequencies need to be implemented, identical distance path and shape at the different locations with several replicates according to the abundance of MPs the region [99, 111], further investigation in the exact amount of water filtered per sample using the PCD and on reducing the LOD caused by the mesh size for a better representation of MPs
2. MPs processing: Although not a focus in this study, further investigation of recovery rates [115] is needed to understand which laboratory methods is better for the type of plastics you may find and the matrix you are sampling.
3. MPs analysis: HSI is efficient at analysing a vast amount of samples, further implementation of polymers in the spectral database should be done and further optimisation on the LOQ of HSI

A multi-matrix sampling could be the next step for these RAPs since less manpower and cost are used for the PCD, and more time and money can be investigated by looking at MPs concentration in the water column and in the sediment. This will help future research to understand the pathways of MPs and paint MPs representativeness without underestimating the abundance of MPs in a marine ecosystem. Pasquier et al. (2023) [109] combined its automated device with an in-situ pump for sediments showing a higher MPs concentration in total compared to only surface water measurement. Combining a multi-matrix sampling with an observational pyramid experiment [151] would be ideal to have ground truth data for MPs abundance and KEVs data to correlate any dynamics that could help predict MPs distribution in the future.

Modellers are noticing the need for more ground truth data [66, 152, 153] to map and predict MPs distribution and help guide policymakers for the implementation of the monitoring framework and guided solutions to reduce marine plastic pollution in the ocean [154, 155, 70, 72] as it is now considered a global planetary threat to humanity [49].

CONCLUSION

Implementing PCD and HSI as a part of RAPs was shown to increase the representativeness of MPs detection and quantification in the marine environment. While PCD helped to increase reproducibility and decrease the probability of operator bias, HSI reduced drastically the analysis time which allows for high sample throughput. While HSI was validated by the FTIR, showing similar MPs concentrations in Runde, limitations with the HSI method keep the TRLs to the applied research stage, suggesting further optimization of the technology, including classification of shape and implementation of more polymer types to the spectral database. Nonetheless, this proposed workflow for MPs sampling and analysis enabled a positive correlation between MPs abundance and wind speed at a specific location. Allowing future research towards RAPS using PCD and HSI will help future MPs research with regards to monitoring multi-matrix MPs distribution, understanding additive effects of KEVs, increasing ground truth data spatially and temporally for fate and prediction models, and providing more evidence for ecotoxicological risk assessments.

REFERENCES

- [1] Amanda Reichelt-Brushett. *Marine Pollution – Monitoring, Management and Mitigation*. Springer Nature, May 2023. ISBN: 978-3-031-10127-4.
- [2] Will Steffen, Paul J Crutzen, John R McNeill, et al. “The Anthropocene: are humans now overwhelming the great forces of nature”. In: *Ambio-Journal of Human Environment Research and Management* 36.8 (2007), pp. 614–621.
- [3] R. Johnston, ed. *Marine pollution*. London ; New York: Academic Press, 1976. ISBN: 978-0-12-387650-8.
- [4] David I Stern. “The role of energy in economic growth”. In: *Annals of the New York Academy of Sciences* 1219.1 (2011), pp. 26–51.
- [5] Philip H Smith. “Plastics come of age”. In: *Scientific American* 152.1 (1935), pp. 5–7.
- [6] Winnie WY Lau et al. “Evaluating scenarios toward zero plastic pollution”. In: *Science* 369.6510 (2020), pp. 1455–1461.
- [7] Stephanie B Borrelle et al. “Predicted growth in plastic waste exceeds efforts to mitigate plastic pollution”. In: *Science* 369.6510 (2020), pp. 1515–1518.
- [8] A. L. Andrady, ed. *Plastics and the ocean: origin, characterization, fate, and impacts*. Hoboken, NJ: Wiley, 2022. ISBN: 978-1-119-76840-1.
- [9] G. G. N. Thushari and J. D. M. Senevirathna. “Plastic pollution in the marine environment”. In: *Heliyon* 6.8 (2020).
- [10] Amy Lusher, Peter Hollman, and Jeremy Mendoza-Hill. *Microplastics in fisheries and aquaculture: status of knowledge on their occurrence and implications for aquatic organisms and food safety*. FAO, 2017.
- [11] Luc Van Hoof et al. “Food from the ocean; towards a research agenda for sustainable use of our oceans’ natural resources”. In: *Marine Policy* 105 (2019), pp. 44–51.
- [12] Rahim Sadigov et al. “Rapid growth of the world population and its socioeconomic results”. In: *The Scientific World Journal* 2022 (2022).
- [13] Chris Walkinshaw et al. “Microplastics and seafood: lower trophic organisms at highest risk of contamination”. In: *Ecotoxicology and Environmental Safety* 190 (2020), p. 110066.
- [14] Mohd Shahnawaz et al., eds. *Impact of plastic waste on the marine biota*. Singapore: Springer, 2022. ISBN: 9789811654022.

REFERENCES

- [15] Viola Fischer et al. “Plastic pollution of the Kuril–Kamchatka Trench area (NW pacific)”. In: *Deep Sea Research Part II: Topical Studies in Oceanography* 111 (2015), pp. 399–405.
- [16] Róisién Nash et al. “Deep Sea Microplastic Pollution Extends Out to Sediments in the Northeast Atlantic Ocean Margins”. In: *Environmental Science & Technology* 57.1 (2022), pp. 201–213.
- [17] X Peng et al. “Microplastics contaminate the deepest part of the world’s ocean”. In: *Geochemical Perspectives Letters* 9.1 (2018), pp. 1–5.
- [18] Marcus Eriksen et al. “Plastic pollution in the world’s oceans: more than 5 trillion plastic pieces weighing over 250,000 tons afloat at sea”. In: *PloS one* 9.12 (2014), e111913.
- [19] Laurent Lebreton. “The status and fate of oceanic garbage patches”. In: *Nature Reviews Earth & Environment* 3.11 (2022), pp. 730–732.
- [20] Melanie Bergmann et al. “High quantities of microplastic in Arctic deep-sea sediments from the HAUSGARTEN observatory”. In: *Environmental science & technology* 51.19 (2017), pp. 11000–11010.
- [21] Gabriella Caruso et al. “Plastic occurrence, sources, and impacts in Antarctic environment and biota”. In: *Water Biology and Security* 1.2 (2022), p. 100034.
- [22] Marcus Eriksen et al. “Mitigation strategies to reverse the rising trend of plastics in Polar Regions”. In: *Environment international* 139 (2020), p. 105704.
- [23] Maria Cristina Fossi et al. “Impacts of marine litter on cetaceans: a focus on plastic pollution”. In: *Marine mammal ecotoxicology*. Elsevier, 2018, pp. 147–184.
- [24] Kelsey Richardson et al. “Building evidence around ghost gear: Global trends and analysis for sustainable solutions at scale”. In: *Marine pollution bulletin* 138 (2019), pp. 222–229.
- [25] Robson G Santos, Gabriel E Machovsky-Capuska, and Ryan Andrades. “Plastic ingestion as an evolutionary trap: Toward a holistic understanding”. In: *Science* 373.6550 (2021), pp. 56–60.
- [26] Outi Setälä, Vivi Fleming-Lehtinen, and Maiju Lehtiniemi. “Ingestion and transfer of microplastics in the planktonic food web”. In: *Environmental pollution* 185 (2014), pp. 77–83.
- [27] Michaela E Miller et al. “Assessment of microplastic bioconcentration, bioaccumulation and biomagnification in a simple coral reef food web”. In: *Science of The Total Environment* 858 (2023), p. 159615.
- [28] LJ Zantis et al. “Assessing microplastic exposure of large marine filter-feeders”. In: *Science of The Total Environment* 818 (2022), p. 151815.
- [29] Stephanie L Wright and Frank J Kelly. “Plastic and human health: a micro issue?” In: *Environmental science & technology* 51.12 (2017), pp. 6634–6647.
- [30] Heather A Leslie et al. “Discovery and quantification of plastic particle pollution in human blood”. In: *Environment international* 163 (2022), p. 107199.

REFERENCES

- [31] Livia Cabernard et al. “Growing environmental footprint of plastics driven by coal combustion”. In: *Nature Sustainability* 5.2 (2022), pp. 139–148.
- [32] Matthew MacLeod et al. “The global threat from plastic pollution”. In: *Science* 373.6550 (2021), pp. 61–65.
- [33] Enrico Pirotta et al. “Understanding the combined effects of multiple stressors: A new perspective on a longstanding challenge”. In: *Science of the Total Environment* 821 (2022), p. 153322.
- [34] Mark P Simmonds. “Marine mammals and multiple stressors: implications for conservation and policy”. In: *Marine mammal ecotoxicology*. Elsevier, 2018, pp. 459–470.
- [35] Robert J. Young and Peter A. Lovell. *Introduction to Polymers*. en. CRC Press, June 2011. ISBN: 978-1-4398-9415-6.
- [36] Charles E Carraher Jr. *Introduction to polymer chemistry*. CRC press, 2012.
- [37] Baljit Singh and Nisha Sharma. “Mechanistic implications of plastic degradation”. In: *Polymer Degradation and Stability* 93 (Mar. 2008), pp. 561–584. DOI: 10.1016/j.polymdegradstab.2007.11.008.
- [38] Anthony L Andrady. “The plastic in microplastics: A review”. In: *Marine pollution bulletin* 119.1 (2017), pp. 12–22.
- [39] Keith J Saunders. *Organic polymer chemistry: an introduction to the organic chemistry of adhesives, fibres, paints, plastics and rubbers*. Springer Science & Business Media, 2012.
- [40] *Plastics - the Facts 2022 • Plastics Europe*. en-GB. URL: <https://plasticseurope.org/knowledge-hub/plastics-the-facts-2022-2/> (visited on 07/08/2023).
- [41] Ramona Marina Grigorescu et al. “Waste electrical and electronic equipment: a review on the identification methods for polymeric materials”. In: *Recycling* 4.3 (2019), p. 32.
- [42] Natalie S. Rudolph, Raphael Kiesel, and Chuanchom Aumanate. *Understanding plastics recycling: economic, ecological, and technical aspects of plastic waste handling*. Cincinnati : Munich: Hanser Publishers ; Hanser Publications, 2017. ISBN: 978-1-56990-676-7.
- [43] VR Sastri. “Chapter 3-Materials Used in Medical Devices. Plastics in Medical Devices”. In: Boston: William Andrew Publishing, 2010.
- [44] Delilah Lithner, Åke Larsson, and Göran Dave. “Environmental and health hazard ranking and assessment of plastic polymers based on chemical composition”. In: *Science of the total environment* 409.18 (2011), pp. 3309–3324.
- [45] Helene Wiesinger, Zhanyun Wang, and Stefanie Hellweg. “Deep dive into plastic monomers, additives, and processing aids”. In: *Environmental science & technology* 55.13 (2021), pp. 9339–9351.
- [46] John Murphy. *Additives for plastics handbook*. Elsevier, 2001.
- [47] Erik Hansen et al. “Hazardous substances in plastic materials”. In: *COWI in cooperation with Danish Technological Institute* (2013), pp. 7–8.

REFERENCES

- [48] Zhanyun Wang and Antonia Praetorius. “Integrating a chemicals perspective into the global plastic treaty”. In: *Environmental Science & Technology Letters* 9.12 (2022), pp. 1000–1006.
- [49] Hans Peter H Arp et al. “Weathering plastics as a planetary boundary threat: exposure, fate, and hazards”. In: *Environmental science & technology* 55.11 (2021), pp. 7246–7255.
- [50] Linda A Amaral-Zettler, Erik R Zettler, and Tracy J Mincer. “Ecology of the plastisphere”. In: *Nature Reviews Microbiology* 18.3 (2020), pp. 139–151.
- [51] Hui Ma et al. “Microplastics in aquatic environments: Toxicity to trigger ecological consequences”. In: *Environmental Pollution* 261 (2020), p. 114089.
- [52] Christina Biamis, Kieran O’Driscoll, and Gary Hardiman. “Microplastic toxicity: A review of the role of marine sentinel species in assessing the environmental and public health impacts”. In: *Case Studies in Chemical and Environmental Engineering* 3 (2021), p. 100073.
- [53] Elitza S Germanov et al. “Microplastics on the menu: plastics pollute Indonesian manta ray and whale shark feeding grounds”. In: *Frontiers in Marine Science* 6 (2019), p. 679.
- [54] Courtney Arthur, Joel E Baker, and Holly A Bamford, eds. *Proceedings of the International Research Workshop on the Occurrence, Effects, and Fate of Microplastic Marine Debris*. National Oceanic and Atmospheric Administration (NOAA), 2009.
- [55] *GESAMP*. International Maritime Organisation, 2015.
- [56] Fan Liu et al. “Shapes of Hyperspectral Imaged Microplastics”. In: *Environmental Science & Technology* 57.33 (2023), pp. 12431–12441.
- [57] Roberto Rosal. “Morphological description of microplastic particles for environmental fate studies”. In: *Marine Pollution Bulletin* 171 (2021), p. 112716.
- [58] João PGL Frias et al. “Floating microplastics in a coastal embayment: A multifaceted issue”. In: *Marine Pollution Bulletin* 158 (2020), p. 111361.
- [59] Carlos Edo et al. “Honeybees as active samplers for microplastics”. In: *Science of The Total Environment* 767 (2021), p. 144481.
- [60] Stefano Magni et al. “The fate of microplastics in an Italian Wastewater Treatment Plant”. In: *Science of the total environment* 652 (2019), pp. 602–610.
- [61] Martin GJ Löder and Gunnar Gerdts. “Methodology used for the detection and identification of microplastics—a critical appraisal”. In: *Marine anthropogenic litter* (2015), pp. 201–227.
- [62] Ludovica Fiore et al. “Classification and distribution of freshwater microplastics along the Italian Po river by hyperspectral imaging”. In: *Environmental Science and Pollution Research* 29.32 (2022), pp. 48588–48606.
- [63] Hua Zhang. “Transport of microplastics in coastal seas”. In: *Estuarine, Coastal and Shelf Science* 199 (2017), pp. 74–86.

REFERENCES

- [64] Atsuhiko Isobe et al. “Selective transport of microplastics and mesoplastics by drifting in coastal waters”. In: *Marine pollution bulletin* 89.1-2 (2014), pp. 324–330.
- [65] Tobias Kukulka et al. “The effect of wind mixing on the vertical distribution of buoyant plastic debris”. In: *Geophysical research letters* 39.7 (2012).
- [66] Yanfang Li, Hua Zhang, and Cheng Tang. “A review of possible pathways of marine microplastics transport in the ocean”. In: *Anthropocene Coasts* 3.1 (2020), pp. 6–13.
- [67] *Marine Microplastics*. en. June 2021. URL: <https://www.ncei.noaa.gov/products/microplastics> (visited on 08/14/2023).
- [68] Anthony L Andrady. “Microplastics in the marine environment”. In: *Marine pollution bulletin* 62.8 (2011), pp. 1596–1605.
- [69] Matthew Cole et al. “Microplastics as contaminants in the marine environment: a review”. In: *Marine Pollution Bulletin* 62.12 (2011), pp. 2588–2597.
- [70] *GESAMP*. International Maritime Organisation, 2019.
- [71] A Unep and INTERPOL RAPID RESPONSE ASSESSMENT. “The Rise of Environmental Crime”. In: *Nairobi: UNEP* (2016).
- [72] Amy L Lusher et al. “Moving forward in microplastic research: A Norwegian perspective”. In: *Environment International* 157 (2021), p. 106794.
- [73] Jennifer F Provencher et al. “Proceed with caution: the need to raise the publication bar for microplastics research”. In: *Science of the Total Environment* 748 (2020), p. 141426.
- [74] Julie Masura et al. “Laboratory Methods for the Analysis of Microplastics in the Marine Environment: Recommendations for quantifying synthetic particles in waters and sediments.” In: (2015).
- [75] Shiye Zhao et al. “Limitations for microplastic quantification in the ocean and recommendations for improvement and standardization”. In: *Microplastic contamination in aquatic environments*. Elsevier, 2018, pp. 27–49.
- [76] Andrea Faltynkova, Geir Johnsen, and Martin Wagner. “Hyperspectral imaging as an emerging tool to analyze microplastics: a systematic review and recommendations for future development”. In: *Microplastics and Nanoplastics* 1.1 (2021), pp. 1–19.
- [77] Setyo Budi Kurniawan et al. “Current state of marine plastic pollution and its technology for more eminent evidence: a review”. In: *Journal of cleaner production* 278 (2021), p. 123537.
- [78] Lei Mai et al. “A review of methods for measuring microplastics in aquatic environments”. In: *Environmental Science and Pollution Research* 25 (2018), pp. 11319–11332.
- [79] Susanne M. Brander et al. “Sampling and quality assurance and quality control: a guide for scientists investigating the occurrence of microplastics across matrices”. In: *Applied Spectroscopy* 74.9 (2020). Publisher: Society for Applied Spectroscopy, pp. 1099–1125.

REFERENCES

- [80] Gabriel Pasquier et al. “Manta net: The golden method for sampling surface water microplastics in aquatic environments”. In: *Frontiers in Environmental Science* 10 (2022), p. 811112.
- [81] Saif Uddin et al. “Standardized protocols for microplastics determinations in environmental samples from the Gulf and marginal seas”. In: *Marine Pollution Bulletin* 158 (2020), p. 111374.
- [82] Livia Cabernard et al. “Comparison of Raman and Fourier transform infrared spectroscopy for the quantification of microplastics in the aquatic environment”. In: *Environmental science & technology* 52.22 (2018), pp. 13279–13288.
- [83] Jana Weisser et al. “The identification of microplastics based on vibrational spectroscopy data—A critical review of data analysis routines”. In: *TrAC Trends in Analytical Chemistry* 148 (2022), p. 116535.
- [84] Andrea Faltynkova and Martin Wagner. “Developing and testing a workflow to identify microplastics using near infrared hyperspectral imaging”. In: *Chemosphere* (2023), p. 139186.
- [85] Stefano Aliani et al. “Reproducible pipelines and readiness levels in plastic monitoring”. In: *Nature Reviews Earth & Environment* 4.5 (2023), pp. 290–291.
- [86] Artur Zolich et al. “Survey on communication and networks for autonomous marine systems”. In: *Journal of Intelligent & Robotic Systems* 95 (2019), pp. 789–813.
- [87] Gabriel Pasquier et al. “An innovative approach for microplastic sampling in all surface water bodies using an aquatic drone”. In: *Helvion* 8.11 (2022).
- [88] Artur Zolich et al. “Portable Catamaran Drone—an uncrewed sampling vehicle for micro-plastics and aquaculture research”. In: *OCEANS 2022, Hampton Roads*. IEEE. 2022, pp. 1–6.
- [89] Alexander FH Goetz et al. “Imaging spectrometry for earth remote sensing”. In: *science* 228.4704 (1985), pp. 1147–1153.
- [90] Silvia Serranti et al. “Characterization of microplastic litter from oceans by an innovative approach based on hyperspectral imaging”. In: *Waste Management* 76 (2018), pp. 117–125.
- [91] Jiajia Shan et al. “Simple and rapid detection of microplastics in seawater using hyperspectral imaging technology”. In: *Analytica Chimica Acta* 1050 (2019), pp. 161–168.
- [92] Cristiane Vidal and Celio Pasquini. “A comprehensive and fast microplastics identification based on near-infrared hyperspectral imaging (HSI-NIR) and chemometrics”. In: *Environmental pollution* 285 (2021), p. 117251.
- [93] Catherine E Deschênes et al. “Unmanned vehicle and hyperspectral imager for a more rapid microplastics sampling and analysis”.
- [94] Tycho Anker-Nilssen et al. “Key-site monitoring on Runde in 2008”. In: (2009).
- [95] Tycho Anker-Nilssen et al. “Key-site monitoring in Norway 2020, including Svalbard and Jan Mayen”. In: *SEAPOP Short Report* (2021), pp. 1–2021.

REFERENCES

- [96] Glaucia M Fragoso et al. “Contrasting phytoplankton-zooplankton distributions observed through autonomous platforms, in-situ optical sensors and discrete sampling”. In: *Plos one* 17.9 (2022), e0273874.
- [97] Trygve O Fossum et al. “Toward adaptive robotic sampling of phytoplankton in the coastal ocean”. In: *Science Robotics* 4.27 (2019), eaav3041.
- [98] Roald Sætre and Havforskningsinstituttet (Norway), eds. *The Norwegian coastal current: oceanography and climate*. OCLC: ocn123362351. Trondheim: Tapir Academic Press, 2007. ISBN: 978-82-519-2184-8.
- [99] Andrea Faltynkova et al. “Use of an uncrewed surface vehicle and near infrared hyperspectral imaging for sampling and analysis of aquatic microplastics”. submitted.
- [100] Fan Liu et al. “Microplastics in urban and highway stormwater retention ponds”. In: *Science of the Total Environment* 671 (2019), pp. 992–1000.
- [101] Caroline A Schneider, Wayne S Rasband, and Kevin W Eliceiri. “NIH Image to ImageJ: 25 years of image analysis”. In: *Nature methods* 9.7 (2012), pp. 671–675.
- [102] Magnus Själander et al. “EPIC: An energy-efficient, high-performance GPGPU computing research infrastructure”. In: *arXiv preprint arXiv:1912.05848* (2019).
- [103] Charlotte Lefebvre. “Distribution spatiale et temporelle des microplastiques et particules anthropiques au sein d’une lagune côtière mésotidale, le Bassin d’Arcachon. Approche multi-compartiments.” PhD thesis. Université de Bordeaux, 2022.
- [104] Amy L. Lusher et al. “Isolation and extraction of microplastics from environmental samples: an evaluation of practical approaches and recommendations for further harmonization”. In: *Applied Spectroscopy* 74.9 (2020). Publisher: Society for Applied Spectroscopy, pp. 1049–1065.
- [105] Win Cowger et al. “Microplastic spectral classification needs an open source community: open specy to the rescue!” In: *Analytical Chemistry* 93.21 (2021), pp. 7543–7548.
- [106] Amanda L Dawson et al. “Taking control of microplastics data: A comparison of control and blank data correction methods”. In: *Journal of Hazardous Materials* 443 (2023), p. 130218.
- [107] Charlotte Hung et al. “Methods matter: methods for sampling microplastic and other anthropogenic particles and their implications for monitoring and ecological risk assessment”. In: *Integrated environmental assessment and management* 17.1 (2021), pp. 282–291.
- [108] Tania Montoto-Martínez et al. “Comparison between the traditional Manta net and an innovative device for microplastic sampling in surface marine waters”. In: *Marine Pollution Bulletin* 185 (2022), p. 114237.
- [109] Gabriel Pasquier et al. “Vertical distribution of microplastics in a river water column using an innovative sampling method”. In: *Environmental Monitoring and Assessment* 195.11 (2023), p. 1302.

REFERENCES

- [110] Chelsea M Rochman et al. “Local monitoring should inform local solutions: morphological assemblages of microplastics are similar within a pathway, but relative total concentrations vary regionally”. In: *Environmental Science & Technology* 56.13 (2022), pp. 9367–9378.
- [111] Mamoru Tanaka, Tomoya Kataoka, and Yasuo Nihei. “Variance and precision of microplastic sampling in urban rivers”. In: *Environmental Pollution* 310 (2022), p. 119811.
- [112] Phillip Cassey and Tim M Blackburn. “Reproducibility and repeatability in ecology”. In: *BioScience* 56.12 (2006), pp. 958–959.
- [113] Amy L. Lusher et al. “Is it or isn’t it: the importance of visual classification in microplastic characterization”. In: *Applied spectroscopy* 74.9 (2020). Publisher: Society for Applied Spectroscopy, pp. 1139–1153.
- [114] Magnus S Nerheim and Amy L Lusher. “Investigating microsized anthropogenic particles in Norwegian fjords using opportunistic nondisruptive sampling”. In: *Anthropocene Coasts* 3.1 (2020), pp. 76–85.
- [115] Chloe Way et al. “Evidence of underestimation in microplastic research: a meta-analysis of recovery rate studies”. In: *Science of the Total Environment* 805 (2022), p. 150227.
- [116] Therese M Karlsson et al. “Comparison between manta trawl and in situ pump filtration methods, and guidance for visual identification of microplastics in surface waters”. In: *Environmental science and pollution research* 27 (2020), pp. 5559–5571.
- [117] Yutaka Michida et al. “Guidelines for Harmonizing Ocean Surface Microplastic Monitoring Methods. Version 1.1.” In: (2019).
- [118] Julia PS Carvalho, Thaianie S Silva, and Monica F Costa. “Distribution, characteristics and short-term variability of microplastics in beach sediment of Fernando de Noronha Archipelago, Brazil”. In: *Marine Pollution Bulletin* 166 (2021), p. 112212.
- [119] Christopher Dibke, Marten Fischer, and Barbara M Scholz-Böttcher. “Microplastic mass concentrations and distribution in German bight waters by pyrolysis–gas chromatography–mass spectrometry/thermochemolysis reveal potential impact of marine coatings: do ships leave skid marks?” In: *Environmental science & technology* 55.4 (2021), pp. 2285–2295.
- [120] Beverley Henry, Kirsi Laitala, and Ingun Grimstad Klepp. “Microfibres from apparel and home textiles: Prospects for including microplastics in environmental sustainability assessment”. In: *Science of the total environment* 652 (2019), pp. 483–494.
- [121] Penelope K Lindeque et al. “Are we underestimating microplastic abundance in the marine environment? A comparison of microplastic capture with nets of different mesh-size”. In: *Environmental Pollution* 265 (2020), p. 114721.
- [122] Coco Ka Hei Cheung and Christelle Not. “Impacts of extreme weather events on microplastic distribution in coastal environments”. In: *Science of The Total Environment* 904 (2023), p. 166723.

REFERENCES

- [123] Zhiwei Zhang et al. “Coastal ocean dynamics reduce the export of microplastics to the open ocean”. In: *Science of the Total Environment* 713 (2020), p. 136634.
- [124] Golnoush Abbasi et al. “A high-resolution dynamic probabilistic material flow analysis of seven plastic polymers; A case study of Norway”. In: *Environment International* 172 (2023), p. 107693.
- [125] Gabriel Erni-Cassola et al. “Distribution of plastic polymer types in the marine environment; A meta-analysis”. In: *Journal of hazardous materials* 369 (2019), pp. 691–698.
- [126] Kayla C Brignac et al. “Marine debris polymers on main Hawaiian Island beaches, sea surface, and seafloor”. In: *Environmental science & technology* 53.21 (2019), pp. 12218–12226.
- [127] Dongdong Zhang et al. “Microplastic pollution in water, sediment, and fish from artificial reefs around the Ma’an Archipelago, Shengsi, China”. In: *Science of the Total Environment* 703 (2020), p. 134768.
- [128] Sebastian Primpke et al. “Comparison of pyrolysis gas chromatography/mass spectrometry and hyperspectral FTIR imaging spectroscopy for the analysis of microplastics”. In: *Analytical and bioanalytical chemistry* 412 (2020), pp. 8283–8298.
- [129] Melissa R Jung et al. “Validation of ATR FT-IR to identify polymers of plastic marine debris, including those ingested by marine organisms”. In: *Marine pollution bulletin* 127 (2018), pp. 704–716.
- [130] Giuseppe Bonifazi, Giuseppe Capobianco, and Silvia Serranti. “A hierarchical classification approach for recognition of low-density (LDPE) and high-density polyethylene (HDPE) in mixed plastic waste based on short-wave infrared (SWIR) hyperspectral imaging”. In: *Spectrochimica Acta Part A: Molecular and Biomolecular Spectroscopy* 198 (2018), pp. 115–122.
- [131] Lei Su et al. “Global transportation of plastics and microplastics: A critical review of pathways and influences”. In: *Science of The Total Environment* 831 (2022), p. 154884.
- [132] Kristin Andersen et al. “Environmental monitoring at the maren wave power test site off the Island of Runde, Western Norway: Planning and design”. In: *Proceedings of the 8th European Wave and Tidal Energy Conference, Uppsala, Sweden*. 2009, pp. 7–10.
- [133] Øystein Skagseth, Kenneth F Drinkwater, and Emanuele Terrile. “Wind- and buoyancy-induced transport of the Norwegian Coastal Current in the Barents Sea”. In: *Journal of Geophysical Research: Oceans* 116.C8 (2011).
- [134] Toste Tanhua, Sören B Gutekunst, and Arne Biastoch. “A near-synoptic survey of ocean microplastic concentration along an around-the-world sailing race”. In: *Plos one* 15.12 (2020), e0243203.
- [135] Idar Barstad and Sigbjørn Grønås. “Southwesterly flows over southern Norway—Mesoscale sensitivity to large-scale wind direction and speed”. In: *Tellus A: Dynamic Meteorology and Oceanography* 57.2 (2005), pp. 136–152.

REFERENCES

- [136] Florian Faure et al. “An evaluation of surface micro-and mesoplastic pollution in pelagic ecosystems of the Western Mediterranean Sea”. In: *Environmental Science and Pollution Research* 22 (2015), pp. 12190–12197.
- [137] Marie Russell and Lynda Webster. “Microplastics in sea surface waters around Scotland”. In: *Marine Pollution Bulletin* 166 (2021), p. 112210.
- [138] Kuddithamby Gunaalan et al. “Abundance and distribution of microplastics in surface waters of the Kattegat/Skagerrak (Denmark)”. In: *Environmental Pollution* 318 (2023), p. 120853.
- [139] Yong Jiang et al. “Characterization of microplastics in the surface seawater of the South Yellow Sea as affected by season”. In: *Science of the Total Environment* 724 (2020), p. 138375.
- [140] Amy L Lusher et al. “Microplastics in Arctic polar waters: the first reported values of particles in surface and sub-surface samples”. In: *Scientific reports* 5.1 (2015), p. 14947.
- [141] Svetlana Pakhomova et al. “Microplastic variability in subsurface water from the Arctic to Antarctica”. In: *Environmental Pollution* 298 (2022), p. 118808.
- [142] Jakob Bonnevie Cyvin et al. “Macroplastic in soil and peat. A case study from the remote islands of Mausund and Froan landscape conservation area, Norway; implications for coastal cleanups and biodiversity”. In: *Science of the Total Environment* 787 (2021), p. 147547.
- [143] Andrés Cózar et al. “The Arctic Ocean as a dead end for floating plastics in the North Atlantic branch of the Thermohaline Circulation”. In: *Science advances* 3.4 (2017), e1600582.
- [144] Åke Bergman et al. *State of the science of endocrine disrupting chemicals 2012*. World Health Organization, 2013.
- [145] Elysia Jewett et al. “Microplastics and their impact on reproduction—can we learn from the *C. elegans* model?” In: *Frontiers in toxicology* 4 (2022), p. 748912.
- [146] Laura Monclús et al. “Microplastic Ingestion Induces Size-Specific Effects in Japanese Quail”. In: *Environmental Science & Technology* 56.22 (2022), pp. 15902–15911.
- [147] Emily E Burns and Alistair BA Boxall. “Microplastics in the aquatic environment: Evidence for or against adverse impacts and major knowledge gaps”. In: *Environmental toxicology and chemistry* 37.11 (2018), pp. 2776–2796.
- [148] Juan José Alava. “Modeling the bioaccumulation and biomagnification potential of microplastics in a cetacean foodweb of the northeastern pacific: a prospective tool to assess the risk exposure to plastic particles”. In: *Frontiers in Marine Science* 7 (2020), p. 566101.
- [149] Glaucia M Fragoso et al. “Phytoplankton community succession and dynamics using optical approaches”. In: *Continental Shelf Research* 213 (2021), p. 104322.

REFERENCES

- [150] René A Rojas-Luna et al. “Identification, Abundance, and Distribution of Microplastics in Surface Water Collected from Luruaco Lake, Low Basin Magdalena River, Colombia”. In: *Water* 15.2 (2023), p. 344.
- [151] Sivert Bakken et al. “Hypso-1 cubesat: first images and in-orbit characterization”. In: *Remote Sensing* 15.3 (2023), p. 755.
- [152] David Mennekes and Bernd Nowack. “Predicting microplastic masses in river networks with high spatial resolution at country level”. In: *Nature Water* (2023), pp. 1–11.
- [153] Caspar TJ Roebroek et al. “The quest for the missing plastics: Large uncertainties in river plastic export into the sea”. In: *Environmental pollution* 312 (2022), p. 119948.
- [154] Michael S Bank et al. “Global plastic pollution observation system to aid policy”. In: *Environmental Science & Technology* 55.12 (2021), pp. 7770–7775.
- [155] Scott Coffin, Holly Wyer, and JC Leapman. “Addressing the environmental and health impacts of microplastics requires open collaboration between diverse sectors”. In: *PLoS Biology* 19.3 (2021), e3000932.

APPENDICES

A - BATCH PROCESSING OF PHOTOMOSAIC IMAGES

Particle detection in photomosaic images using a batch processing macro in ImageJ [101]

```
run("Set Scale...", "distance=1436.0031 known=69000 pixel=1.101 unit=um");  
run("8-bit");  
  
setOption("BlackBackground", false);  
run("Convert to Mask");  
run("Fill Holes");  
run("Set Measurements...", "feret's display redirect=None decimal=3");  
run("Analyze Particles...", "size=0-Infinity show=Outlines display summarize");  
run("Close");
```

B - STATISTICAL TESTS

Table B.1: Statistical tests: p-value results (Signif. codes: 0 ‘***’ 0.001 ‘**’ 0.01 ‘*’ 0.05 ‘.’ 0.1 ‘ ’ 1)

| Parameters | Tests | (p-value <0.05) |
|---|----------|-----------------|
| Volumes (flowmeter vs robot) | Wilcoxon | 0.000004 *** |
| MPs concentration (FTIR vs HSI) | K-W | 0.2853 |
| MPs concentration with HSI (Locations A vs B) | K-W | 0.0324 . |
| PPs concentration (FTIR vs HSI) | K-W | 0.0343 |
| PPs concentration with HSI (Locations A vs B) | K-W | 0.0903 |
| PEs concentration (FTIR vs HSI) | K-W | 0.859 |
| PEs concentration with HSI (Locations A vs B) | K-W | 0.0834 |
| Size (FTIR vs HSI) | K-W | 0.0067 * |
| Size 500-5000 μm (FTIR vs HSI) | K-W | 0.178 |
| Size with HSI (Location A vs Location B) | K-W | 0.893 |
| MPs concentration vs Days | K-W | 0.00265 * |
| Aug 2 vs 3 | Dunn | 0.0619 |
| Aug 2 vs 4 | Dunn | 0.00238 * |
| Aug 2 vs 5 | Dunn | 1 |
| Aug 3 vs 4 | Dunn | 0.862 |
| Aug 3 vs 5 | Dunn | 0.26 |
| Aug 4 vs 5 | Dunn | 0.0203 . |

C - FIELDWORK DETAILS

C1 - Fieldwork metadata

Table C.1: Summary of the field campaign including PCD information, MPs concentrations, and KEVs data related to each run. Yellow rows correspond to errors in the navigation system. Green rows correspond to entanglement with help in the propellers.

| Date | Start Sampling | Location | Runs | Planned Path (m) | Distance travelled (m) | Duration (s) | Speed (m/s) | Volume from robot (m ³) | Volume from flowmeter (m ³) | MPs concentration (particles / m ³) | Wind (m/s) | Tide (m) |
|------------|----------------|----------|------|------------------|------------------------|--------------|-------------|-------------------------------------|---|---|------------|----------|
| 02/08/2022 | 09:49:23 | A | 1 | 370 | 289 | 460 | 0.629 | 12.9 | 10.6 | 0.094 | 6.9 | 117 |
| 02/08/2022 | 10:14:42 | A | 2 | 370 | 284 | 478 | 0.595 | 12.6 | 12.0 | 0.000 | 6.9 | 130 |
| 02/08/2022 | 11:34:30 | A | 3 | 370 | 315 | 502 | 0.627 | 14.0 | 11.3 | 0.000 | 6.9 | 172 |
| 02/08/2022 | 11:58:12 | A | 4 | 370 | 290 | 507 | 0.573 | 12.9 | 11.3 | 0.000 | 6.9 | 181 |
| 02/08/2022 | 12:26:59 | A | 5 | 370 | 294 | 521 | 0.565 | 13.1 | 11.3 | 0.000 | 10.9 | 179 |
| 02/08/2022 | 12:56:00 | A | 6 | 370 | 233 | 405 | 0.576 | 10.4 | 11.3 | 0.000 | 10.9 | 185 |
| 02/08/2022 | 13:23:00 | A | 7 | 370 | NA | NA | NA | 13.0 | 11.3 | 0.000 | 17.2 | 184 |
| 02/08/2022 | 13:54:39 | A | 8 | 370 | 296 | 507 | 0.583 | 13.1 | 11.3 | 0.000 | 17.2 | 180 |
| 02/08/2022 | 14:26:44 | A | 9 | 370 | 298 | 500 | 0.596 | 13.3 | 11.3 | 0.000 | 14 | 171 |
| 02/08/2022 | 14:56:09 | A | 10 | 370 | 297 | 520 | 0.571 | 13.2 | 11.3 | 0.000 | 14 | 158 |
| 03/08/2022 | 09:03:50 | A | 11 | 680 | 309 | 753 | 0.410 | 13.7 | 3.3 | 0.305 | 12.9 | 88 |
| 03/08/2022 | 09:36:00 | A | 12 | 680 | NA | NA | NA | 26.1 | 16.7 | 0.299 | 12.9 | 106 |
| 03/08/2022 | 10:10:42 | A | 13 | 680 | 580 | 977 | 0.593 | 25.8 | 16.1 | 0.124 | 22.3 | 124 |
| 03/08/2022 | 10:48:12 | A | 14 | 680 | 572 | 956 | 0.599 | 25.4 | 16.5 | 0.787 | 22.3 | 147 |
| 03/08/2022 | 11:29:34 | A | 15 | 680 | 610 | 1014 | 0.602 | 27.1 | 17.5 | 0.285 | 20.3 | 169 |
| 03/08/2022 | 15:02:20 | B | 16 | 600 | 493 | 787 | 0.626 | 11.0 | 7.0 | 0.428 | 19.4 | 185 |
| 03/08/2022 | 15:59:04 | B | 17 | 600 | 437 | 743 | 0.588 | 19.4 | 18.7 | 0.000 | 19.4 | 160 |
| 03/08/2022 | 16:24:28 | B | 18 | 600 | 438 | 748 | 0.586 | 19.5 | 17.4 | 0.000 | 16.4 | 149 |
| 03/08/2022 | 16:48:43 | B | 19 | 600 | 447 | 746 | 0.600 | 19.9 | 17.0 | 0.000 | 16.4 | 134 |
| 04/08/2022 | 09:21:32 | A | 20 | 680 | 6 | 14 | 0.434 | 20.7 | 20.7 | 0.145 | 12.1 | 69 |
| 04/08/2022 | 09:56:01 | A | 21 | 680 | 599 | 980 | 0.611 | 26.7 | 0.0 | 0.096 | 12.1 | 83 |
| 04/08/2022 | 10:25:41 | A | 22 | 680 | 588 | 975 | 0.603 | 26.1 | 20.3 | 0.049 | 9.3 | 92 |
| 04/08/2022 | 10:54:11 | A | 23 | 680 | 602 | 966 | 0.623 | 26.8 | 21.5 | 0.139 | 9.3 | 106 |
| 04/08/2022 | 11:27:19 | A | 24 | 680 | 1202 | 2062 | 0.583 | 17.6 | 17.6 | 0.000 | 14.2 | 128 |
| 04/08/2022 | 12:25:10 | A | 25 | 680 | 374 | 815 | 0.458 | 4.2 | 4.2 | 0.000 | 10.5 | 158 |
| 04/08/2022 | 13:51:40 | A | 26 | 680 | 623 | 1041 | 0.598 | 27.7 | 20.9 | 0.192 | 11.5 | 174 |
| 04/08/2022 | 14:29:01 | A | 27 | 680 | 699 | 1242 | 0.563 | 31.1 | 20.9 | 0.335 | 12.7 | 174 |
| 05/08/2022 | 10:18:57 | B | 28 | 600 | 480 | 759 | 0.556 | 21.3 | 18.3 | 0.055 | 15.4 | 75 |
| 05/08/2022 | 10:25:39 | B | 29 | 600 | 474 | 759 | 0.624 | 21.1 | 19.9 | 0.000 | 15.4 | 77 |
| 05/08/2022 | 10:51:27 | B | 30 | 600 | 503 | 881 | 0.572 | 22.4 | 17.8 | 0.056 | 15.4 | 87 |
| 05/08/2022 | 10:56:38 | B | 31 | 600 | 620 | 1033 | 0.600 | 6.5 | 6.5 | 0.000 | 15.4 | 91 |
| 05/08/2022 | 11:27:51 | B | 32 | 600 | 488 | 844 | 0.578 | 21.7 | 14.2 | 0.000 | 17.3 | 106 |
| 05/08/2022 | 11:33:07 | B | 33 | 600 | 477 | 750 | 0.637 | 20.7 | 20.7 | 0.000 | 17.3 | 106 |
| 05/08/2022 | 11:59:35 | B | 34 | 600 | 482 | 850 | 0.568 | 21.4 | 18.3 | 0.000 | 17.3 | 121 |
| 05/08/2022 | 12:37:55 | B | 35 | 600 | 500 | 850 | 0.588 | 22.2 | 18.6 | 0.000 | 17.4 | 140 |

C2 - Microscope pictures of MPs

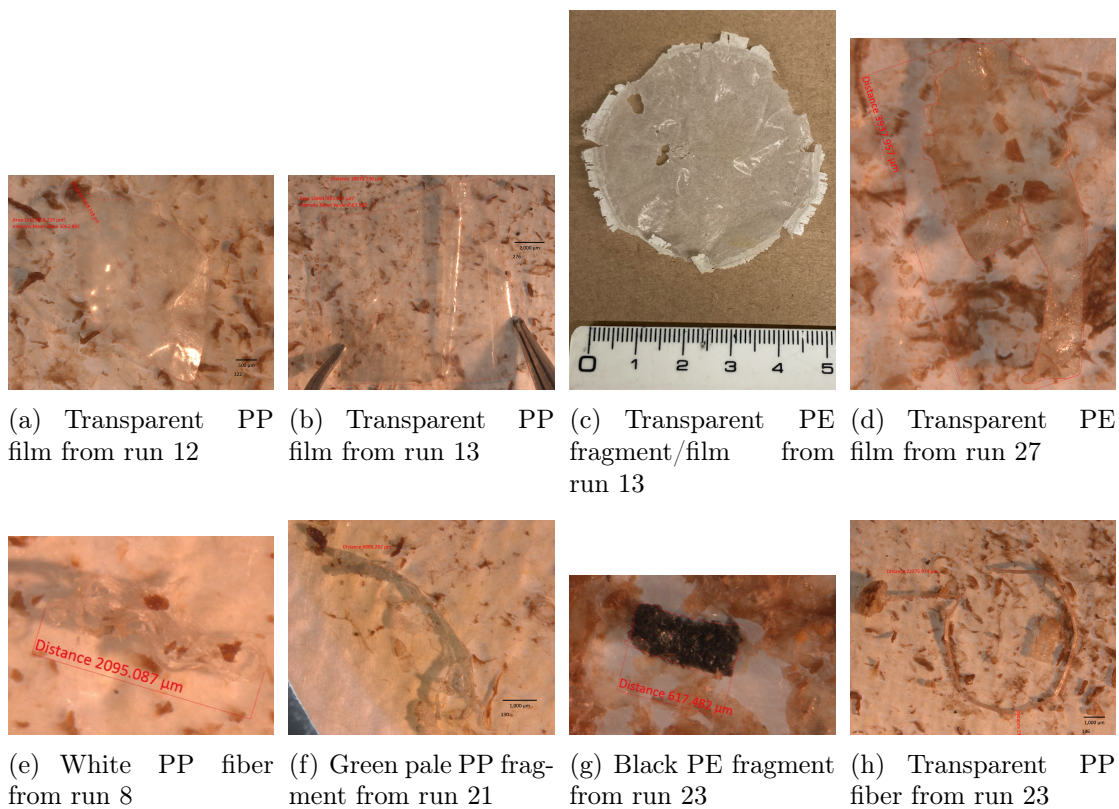


Figure C.1: Examples of MPs detected by visual inspection under the microscope with the FTIR method but missed by the HSI method

C3 - Metadata drive repository for morphological and chemical information on suspected (confirmed and unconfirmed) MPs (> 300 µm) for all samples, blanks, and artificial spiked samples and both instruments (HSI and FTIR) collected at Runde. Microscope pictures are also included.

Click here to access metadata

C4 - Colours distribution in the MPs confirmed by the FTIR method

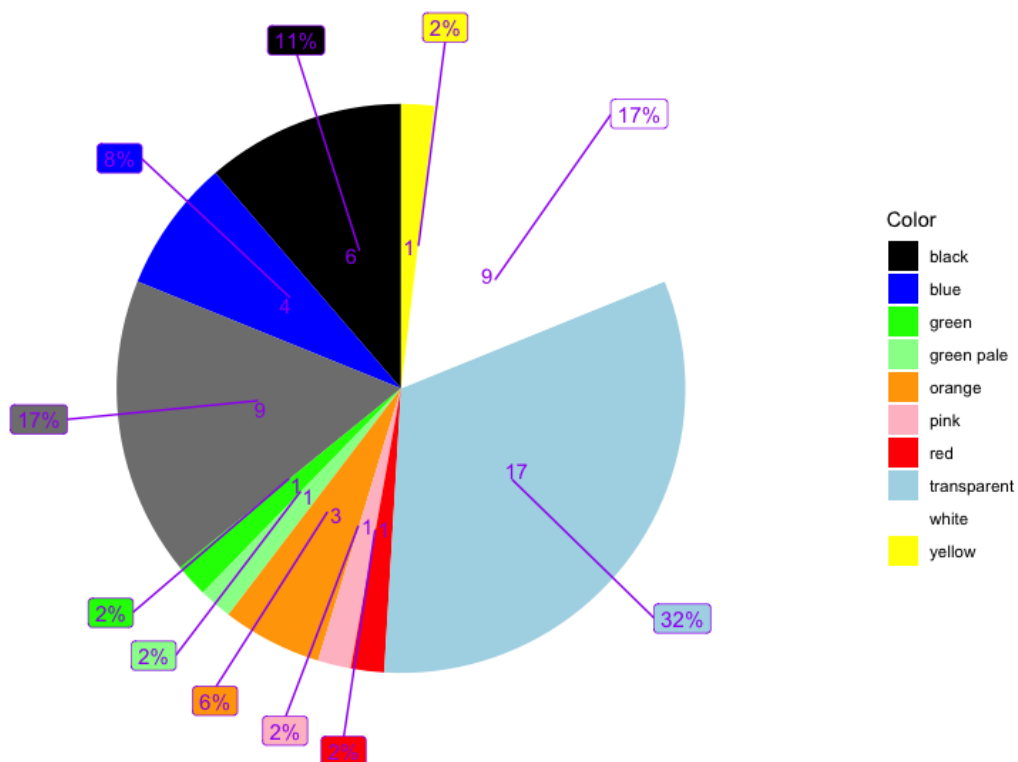


Figure C.2: Colour distribution of samples analyzed under the FTIR method



NTNU

Norwegian University of
Science and Technology